TAMPEREEN TEKNILLINEN YLIOPISTO
TAMPERE UNIVERSITY OF TECHNOLOGY

HESHAM ELGENDI

PERFORMANCE ANALYSIS OF INTERFERENCE MEASUREMENT METHODS FOR LINK ADAPTATION IN 5G NEW RADIO

Master of Science Thesis

Examiner: Prof. Mikko Valkama
Supervisor: M.Sc. Mikko Maenpaa
Examiner and topic approved on 31 May 2018

ABSTRACT

ELGENDI, HESHAM: Performance analysis of interference measurement methods for link adaptation in 5G New Radio
Tampere University of Technology
Master of Science Thesis, 74 pages
December 2018
Master's Degree Program in Information Technology
Major: Communication Systems and Networks
Examiner: Prof. Mikko Valkama
Supervisor: MSc. Mikko Maenpaa

Keywords: 5G NR, link adaptation, channel state information, channel quality indicator, CSI-IM, NZP CSI-RS

5G New Radio (NR) is coming faster than expected with early deployments which take place early 2019. It is more than a new mobile generation that offers higher data rates compared to previous generations, although it's still the main driver. It will enable many new use cases and deployment scenarios that can be put into three main categories: enhanced mobile broad band (eMBB), ultra-reliable low latency communications (URLLC) and massive machine type communications (mMTC).

5G NR aims to further increase frequency resources utilization and efficiency. Cell edge users usually suffer from high levels of interference known as inter-cell interference. This phenomenon results in lower performance for the cell edge users and inefficient utilization of radio resources. Link adaptation techniques aim to increase cell edge performance by exploiting varying channel conditions and interference level at user equipment (UE). In this thesis channel state information (CSI) is studied as an essential part of link adaptation process. Channel quality indicator (CQI) is the main component of CSI reports from UE that gives recommendations about the next transmission modulation order and code rate. The accuracy of reported CQI depends on the accuracy of channel and interference measurements. In this thesis two different interference measurement methods based on two reference signals are studied: CSI interference measurement (CSI-IM) and non-zero power CSI reference signal (NZP CSI-RS). In this thesis performance with different configurable factors, different channel models and UE speeds are considered. Overall system overhead is also studied to give recommendation about the configuration of lower system overhead. Simulation results has shown that CSI-IM based interference measurement is more efficient compared to NZP CSI-RS method and operates well in different channel scenarios and different UE speed. While NZP CS-RS shows sensitivity to frequency selective channels and in higher user mobility cases. On the other hand, from overall system overhead perspective, CSI-IM based configuration is the best solution.

PREFACE

This thesis is an output of collaboration between Nokia Bell Labs and the laboratory of Electronics and Communications Engineering of Tampere University of Technology. I have been part of collective efforts of developing 5G Link level simulator in the past 11 months. The study and results obtained for this thesis are generated through simulations carried out using this simulator.

I would like to express my gratitude to Professor Mikko Valkama for his continuous support, constructive feedback and patience during the development of the thesis. Special thanks to M.Sc. Mikko Maenpaa for his technical support, insights and thoughts that helped me a lot to accomplish this thesis. His guidance was there whenever needed and was always very helpful.

I would like to extend my warmest and sincere thanks to all my colleagues D.Sc. Tero Ihalainen, D.Sc. Toni A. Levanen and M.Sc. Elena Peralta for valuable discussions and great spirit during the entire process.

Many thanks to my family for unconditional love I had. Special thanks to my father, without his support and values he taught me, I will never be here writing these words today.

I am also very grateful to my friends, specially Dr. Ahmad Shalaby for his advices and great discussions we had in different life topics that added a new dimension to my personality, for which I am forever thankful.

Tampere, December 2018

Hesham Elgendi

CONTENTS

LIST OF FIGURES

LIST OF TABLES

ABBREVIATIONS

3GPP	3rd Generation Partnership Project
5G	5th Generation
AMC	Adaptive Modulation and Coding
AWGN	Additive White Gaussian Noise
BLER	Block Error Rate
BPSK	Binary Phase Shift Keying
CDM	Code Division Multiplexing
CP	Cyclic Prefix
CPE	Common Phase Error
CQI	Channel Quality Indicator
CRS	Cell-specific Reference Signal
CSI	Channel State Information
CSI-IM	CSI-Interference Measurement
CSI-RS	CSI-Reference Signal
D/A	Digital to analog converter
DCI	Downlink Control Indicator
DIP	Dominant Interfere Proportion
DMRS	Demodulation Reference Signal
eMBB	Enhanced Mobile Broadband
FDD	Frequency Division Duplexing
FFT/IFFT	Fast Fourier Transform/ Inverse FFT
FG	Frequency Granularity
gNB	gNodeB (5G NR base station)
HARQ	Hybrid Automatic Repeat Request
IM	Interference Measurement
INR	Interference to Noise Ratio
IRC	Interference Rejection Combining
ISI	Inter Symbol Interference
LA	Link Adaptation
LDPC	Low Density Parity Check
LI	Layer Indicator
LTE	Long Term Evolution
MCS	Modulation and Coding scheme
MIMO	Multiple-Input Multiple-output
MMIB	Mean Mutual Information per Bit
MMSE	Minimum Mean Square Error
mMTC	Massive Machine Type Communications
NR	New Radio

NZP	Non-Zero Power CSI-RS
OFDM	Orthogonal Frequency Division Multiplexing
OFDMA	Orthogonal Frequency Division multiple Access
OLLA	Outer Loop Link Adaptation
P/S	Parallel to series
PAPR	Peak to Average Power Ratio
PBCH	Physical Broadcast Channel
PDCCH	Physical Downlink Control Channel
PDSCH	Physical Downlink Shared Channel
PMI	Precoder Matrix Indicator
PRACH	physical Random-Access Channel
PRB	Physical Resource Block
PTRS	Phase Tracking Reference Signal
PUCCH	Physical Uplink Control Channel
PUSCH	Physical Uplink Shared Channel
QAM	Quadrature Amplitude modulation
QPSK	Quadrature Phase Shift Keying
RE	Resource Element
RI	Rank Indicator
RRM	Radio Resource Management
RS	Reference Signal
RSRP	Reference Signal Received Power
S/P	Serial to parallel
SF	Subframes
SINR	Signal to Interference plus Noise Ratio
SNR	Signal to Noise Ratio
TDD	Time Division Duplexing
TDM	Time Division Multiplexing
TP	Throughput
UE	User Equipment
URLLC	Ultra Reliable Low Latency Communications
ZP CSI-RS	Zero Power CSI-RS

SYMBOLS

c	Speed of light
f_c	Carrier frequency
f_d	Maximum doppler spread
f_s	Sampling rate
$\hat{\mathbf{h}}$	Output estimated channel vector of the Wiener filter
$\mathbf{h}(t)_{i,j}$	Channel response vector of transmitted signal from transmit antenna i to receive antenna j
$\mathbf{H}_{\text{interf}}$	Channel response matrix of interfering signal
$h_{raw}(f)$	Raw channel estimate at reference symbol position
$\mathbf{i}(m,t)_{ij}$	Interfering signal vector from interfering gNB m
N	FFT size
$\mathbf{n}(t)_j$	AWGN component vector on receive antenna j
N_c	Number of active subcarriers
N_{cell}	Number of interfering gNBs
N_{cp}	Cyclic prefix number of samples
$\mathbf{R}$	Interference plus noise covariance matrix
$\mathbf{R}_{\text{n}}$	Covariance matrix of interference plus noise component
$\mathbf{R}_y$	Auto-correlation matrix of received signal y
$\mathbf{R}_{yx}$	Cross correlation matrix of the received and transmitted signals
s_{ref}	Transmitted reference symbol
T_c	Coherence time
T_{cp}	Cyclic prefix length
T_u	OFDM Symbol period
v	UE speed
$\mathbf{W}_1$	First Wiener filter coefficients matrix (Frequency direction)
$\mathbf{W}_2$	Second Wiener filter coefficients matrix (Time direction)
$\mathbf{W}_{MMSE}$	MMSE filter coefficients matrix
$\mathbf{x}(t)_i$	Transmitted signal vector from transmit antenna i
x_{interf}	Transmitted interfering symbol
$\mathbf{y}(t)_j$	Received signal vector on receive antenna j
$y_{ref}(f)$	Received reference symbol
Δf	Subcarrier spacing
α	Forgetting factor
$(.)_{\text{S}}$	Denotes a symbol of serving cell
$(.)_{\text{d}}$	Denotes a symbol of dominant interferer
$(.)_{\text{w}}$	Denotes a symbol of serving weaker interferer

1. INTRODUCTION

The demand for voice and data communications has increased exponentially over the last decades. Such increasing demand triggered new mobile access technology every ten years. Data hungry applications, such as online streaming with increasing resolution and viewing time are the driving wheels for the continuous evolutions in the mobile access technologies. UE that supports 4k video streaming will need a data rate of 15.4 Mbps per user [1]. It is expected that the annual mobile traffic will increase to 291.8 exabyte by 2019 [2]. The wireless communications will connect everything and anything in the next years to come. This will affect people's life and society to operate using the existing resources efficiently. 5G NR will be in the heart of this process as it is coming as a new platform of innovations that will redefine many industries and introduce new services.

1.1 5G New Radio overview

The third-generation partnership project (3GPP) has approved the first specification of the new fifth generation radio interface known as 5G New Radio (NR), that is Release 15 by the end of 2017. The first NR deployment will depend on existing LTE network for initial access and mobility management, which known as non-standalone operation and it is expected to take place in 2019. 5G NR will continue to be driven by very high demand for higher data rates, increased overall capacity and better coverage. 5G NR promises to support 10 Gbps peak data rates and 100 Mbps generally in the urban and suburban areas. This implies providing data rates about 10 times compared to the existing wireless technology. However, 5G NR is unlike the previous generations and it offers more than this. For example, 5G NR will support mMTC that requires handling very large number of connected devices operating with minimum energy consumption. For example, a large number of connected sensors that collect different kind of data. This requires possibility for very low-cost devices and operating with extremely low energy to support a 10 years life time battery. Because in some deployment scenarios it is hard to change the battery regularly.

URLLC is another category for new use cases that 5G NR will support. URLLC will enable new services that requires data delivery with very high reliability and at the same time very low latency. It is required to support end to end latency in the order of 1 ms and very low error rate below 10^{-9}. For example, this can enable safer and more autonomous transportation. The first 5G NR specification that is Release 15 will focus on standardizing eMBB and URLLC [3].

Forward compatibility is one important designing principle for the new radio interface, that it can support the future not foreseen yet new use cases and deployment scenarios. Moreover, a self-contained integrated subframe design enables efficient multiplexing of different services on the same network [4]. Enhanced mobile broadband (eMBB) will be enabled by combining different technologies, whereas 3GPP has agreed that 5G NR can operate from below 1GHz up to 52.6 GHz both in licensed and unlicensed spectrum. This allows operating at millimeter-wave (mmWave) frequencies, therefore very large transmission bandwidths can be deployed enabling for higher data rates and system capacity. Although operating in mmWave bands come with price of a very challenging propagation conditions where higher signal attenuation is introduced limiting the network coverage. This can be partially tackled by massive MIMO technologies enabled by very small size of antenna elements. It should be noted that operation at low frequencies will be essential part of 5G NR to provide the basic coverage to the network, while higher frequency bands will be used to support users with very high data demands [3].

1.2 Objective and thesis scope

In this thesis, link level performance of 5G NR downlink data channel is evaluated for UE on the cell edge with interference model. In this model the link between one serving cell and one UE is modeled. Also, two interfering cells are modeled, where based-band signals are generated and added to the received signal at UE according to the defined interference to noise ratio (INR) profile. The serving cell is using link adaptation (LA) techniques to follow channel state information (CSI) reports from UE. CSI consists of channel quality indicator (CQI), precoding matrix index (PMI), CSI-RS resource indicator, layer indication(LI), rank indication (RI) and / or L1-RSRP. However, in this thesis we focus only on CQI as one of the CSI components that reflects average channel conditions and interference levels at UE.

In LA process, transmission settings including for example: modulation scheme and code rate are defined based on reported CQI from UE. LA aims to efficiently utilize the available radio resources and increase system capacity by exploiting the varying channel conditions. In order to calculate CQI, an accurate channel and interference measurements are needed at UE side. In this thesis, the objective is to study different reference signal-based interference measurement and define the most accurate and efficient one. Since the quality of channel and interference measurements needed to calculate CQI strongly affects the quality of LA process, two reference signals are studied in this thesis. First, CSI-interference measurement (CSI-IM) reference signal (RS) where empty resource elements (REs) in subframe of serving cell are defined to collide with the data REs in subframe of interfering cells. Second, Non Zero Power CSI-RS (NZP CSI-RS) where it is scheduled for two purposes, firstly is to get channel measurement and secondly it can be also used to get interference measurement. The performance of previously mentioned RS-based interface measurement is evaluated using different channel models and different

UE speeds. Moreover, in this thesis a performance comparison between two proposed methods are studied trying to answer one question, which RS based interference measurement is more accurate and results in overall best performance taking into consideration the total system overhead. Extensive link level simulations are carried out to conduct this study. The goal is to define the optimal operating configuration that delivers the highest performance and lowest system overhead.

1.3 Thesis structure

In Chapter two, the basic understanding of 5G NR physical layer is introduced. Concepts such as: orthogonal frequency division multiplexing (OFDM) as the main modulation scheme in downlink transmission in NR is introduced. Moreover, DFT- spread OFDM as the uplink modulation scheme, frame structure and flexible numerology are explained. In Chapter three, theoretical framework and fundamentals of this thesis are explained. For instance, LA techniques are explained as an essential tool in any cellular system to efficiently utilize radio resources and improve cell-edge performance. Moreover, CSI reporting is discussed in details. Channel and interference measurements necessary of CQI calculations are introduced. Chapter four, defines simulation assumptions and link level performance of each RS-based interference measurement. Furthermore, A comparison between two interference measurement methods are studied. Overall system overhead analysis for different configurations is also studied. Finally, Chapter five, is thesis conclusion and final remarks.

2. PHYSICAL LAYER OF 5G NR

In this chapter, a basic understanding of 5G NR downlink physical layer is given. 5G NR is more than a new mobile generation with further enhancement in mobile broadband capabilities in terms of high data rates, coverage and capacity. New use cases and deployment scenarios are to be enabled with 5G NR with very low latency and high reliability. Moreover, improved network energy performance and operation in a very high frequency bands where higher bandwidth is available. In this chapter, OFDM is explained as the main waveform used for downlink data transmission for its benefits as a frequency efficient waveform and orthogonality between subcarriers. DFT-S-spread is also introduced as uplink waveform to overcome peak to average power ratio problem inherited in OFDM signal which becomes challenging in uplink transmission. 5G NR will adopt flexible numerology for subcarrier spacings to enable different deployment scenarios. In this chapter, the effect of such flexible numerology on frame structure is explained. Moreover, reference signals, channel coding and physical channels are introduced.

2.1 Orthogonal Frequency Division Multiplexing

In this section, an overview of an OFDM signal is introduced. OFDM is the main modulation scheme in LTE/LTE-advanced and it is chosen to be the successful candidate among many proposed modulation schemes in 5G NR [9]. OFDM signal has very high spectral efficiency that meets 5G NR requirements for very high spectral efficiency. Moreover, OFDM signal is robust to time and frequency channel selectivity by proper choice of subcarrier spacing and cyclic prefix (CP) [5]. OFDM receiver has the lowest complexity compared to all waveforms candidates studied for 5G [11].

Basically, OFDM is a multicarrier transmission intended for high data rate communications to cope against channel selectivity both in time and frequency. Due to increasing demand for higher data rates, more bandwidth is allocated for transmission through the channel. The total allocated bandwidth is divided into very large number of relatively narrowband subcarriers. Each subcarrier is carrying a modulated symbol that is transmitted in parallel into the channel. These subcarriers should be orthogonal to each other, so that modulated symbols can be detected properly at the receiver [6]. Orthogonal subcarriers are overlapping in frequency domain, this structure provides higher spectral efficiency compared to conventional frequency division multiplexing (FDM) scheme, this can be seen in Figure 1.

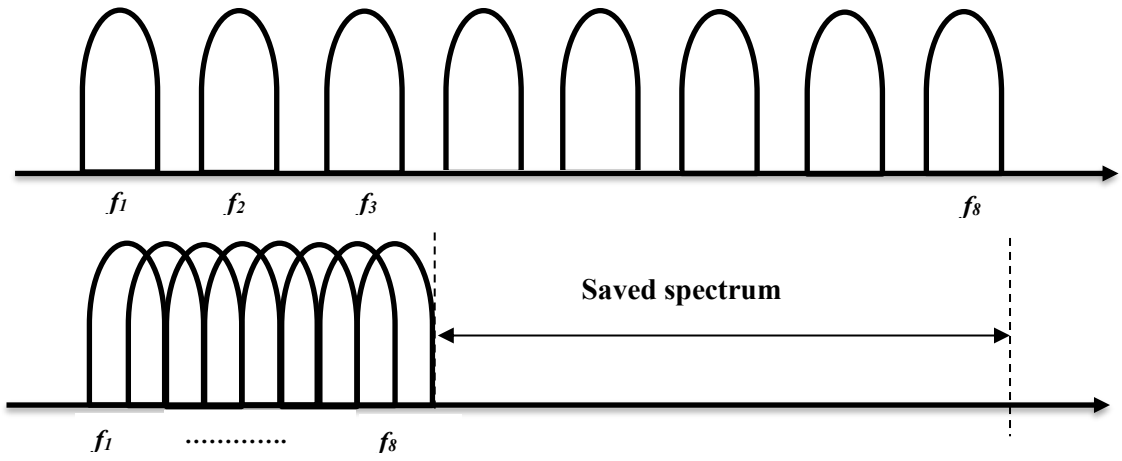

Figure 1. *OFDM spectral efficiency*

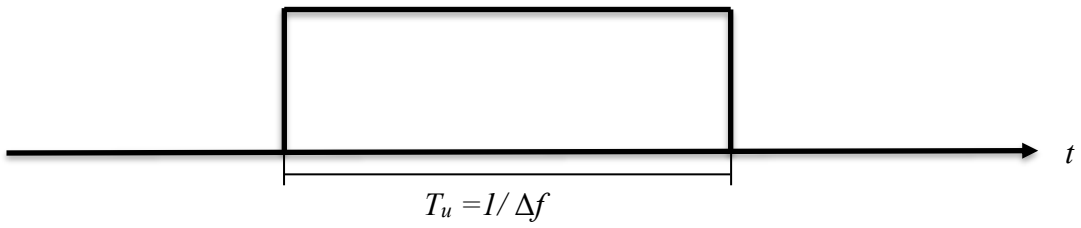

Figure 2. *Time domain pulse shape of one OFDM subcarrier*

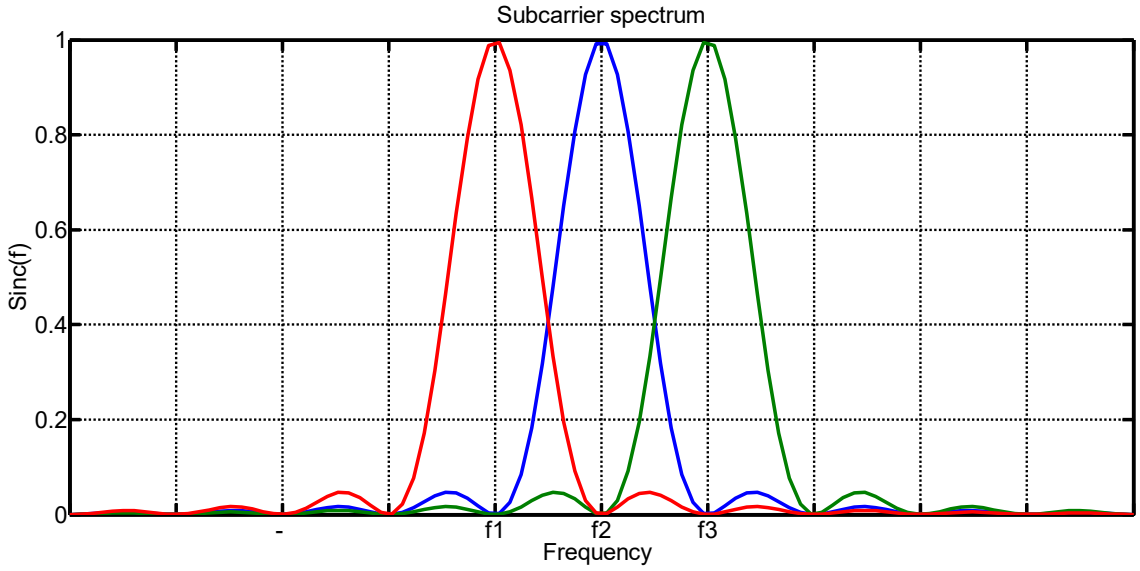

Figure 3. *Orthogonality of OFDM subcarriers in frequency domain*

The frequency separation Δf, between subcarriers, i.e., subcarrier spacing is $\Delta f = 1/T_u$, where T_u is subcarrier symbol period, thus subcarrier spacing is equal to symbol rate $1/T_u$. A basic rectangular pulse shape is used in OFDM systems with time width of T_u, as shown

in Figure 2, resulting in a spectrum of individual subcarrier has the shape of sinc function as shown in Figure 3. Figure 3, shows the orthogonality between subcarriers where at the peak amplitude of each subcarrier there is a zero amplitude (null) for other subcarriers.

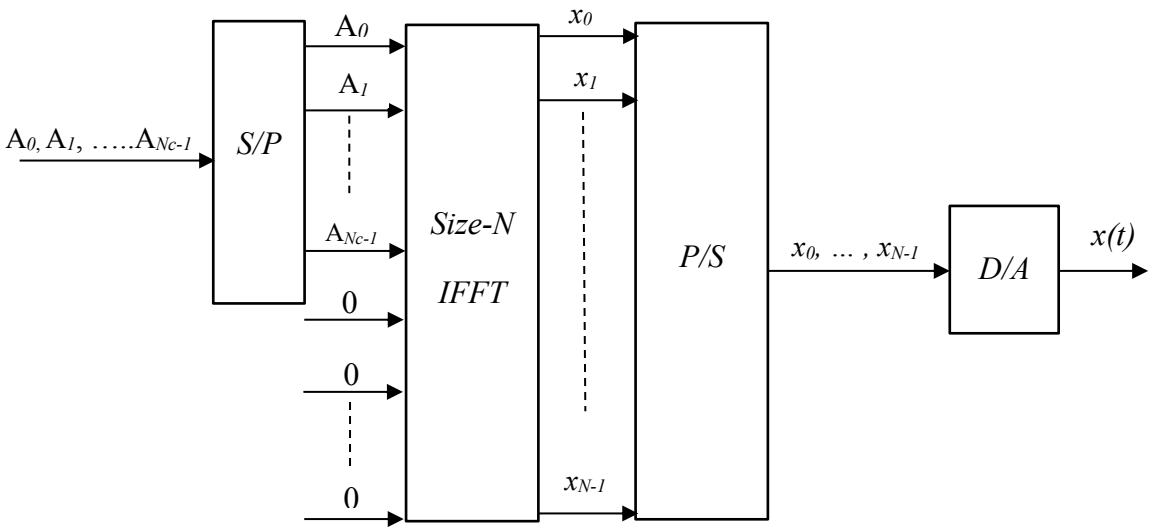

Figure 4. *OFDM signal modulation*

An OFDM signal can be generated through a bank of modulators. Each modulator corresponds to each subcarrier which has proven to be not practically feasible. Alternatively, a practical low complexity implementation using computationally efficient Fast Fourier Transform (FFT) is used. In the transmitter side, the upcoming data symbols N_c are mapped to the input bins of Inverse Fast Fourier Transform (IFFT). Therefore, OFDM transmission is block based, where one block carriers a maximum of N_c data symbols.

In Figure 4, basic OFDM transmitter is introduced. The upcoming N_c modulated data symbols are mapped to input bins of size-N IFFT block, with the rest N-N_c bins are extended with zeros. The N output samples are converted into serial stream after parallel to serial block then time domain signal $x(t)$ is generated after digital to analog converter. It is worth noting that, the choice of IFFT size N should be equal to 2^m for some integer m, so that the efficient radix-2 IFFT can be implemented. Moreover, the choice of N should exceed N_c, with sufficient margin so that the sampling theorem is fulfilled [8].

In the receiver side, OFDM signal demodulation is processed with FFT block. It can be seen in Figure 5, that received signal is sampled with sampling rate $f_s = N \times \Delta f$, and mapped to size-N FFT bins. The unused bins are discarded obtaining the N_c data symbols and forwarded to further processing.

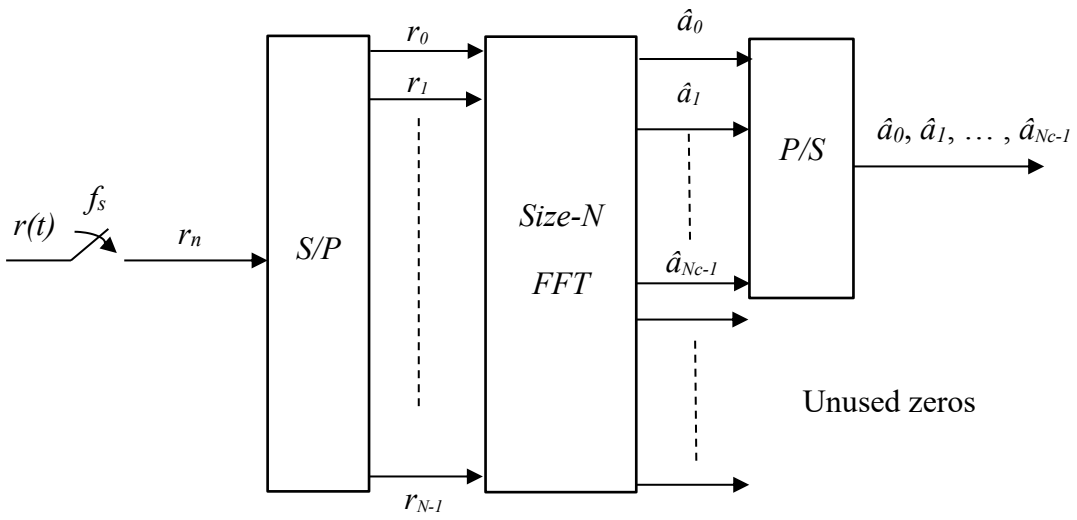

Figure 5. *OFDM signal demodulation*

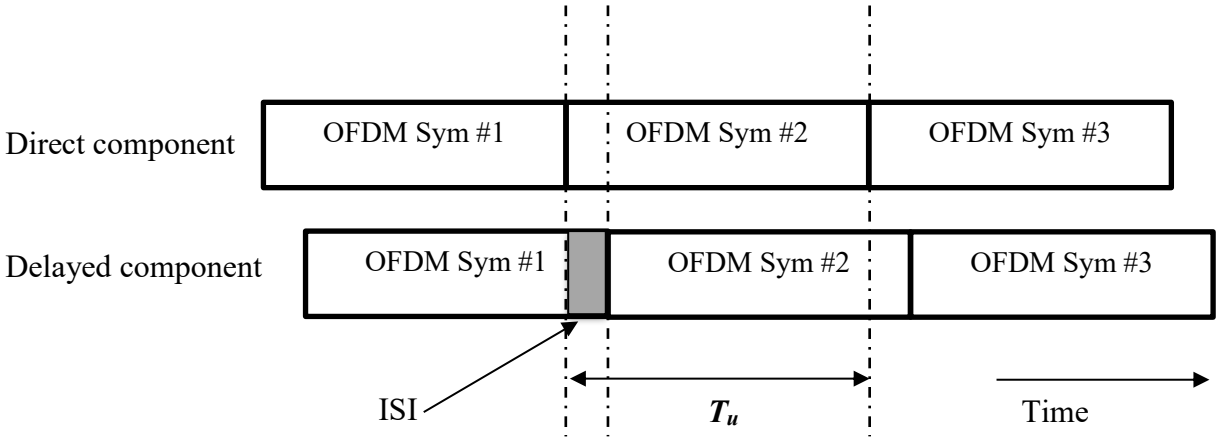

Figure 6. *Inter-symbol interference in multi-path propagation.*

Cyclic prefix

OFDM signals are very sensitive to time dispersive nature of the frequency channels that leads to loss of orthogonality between subcarriers. Time dispersive nature of radio channel stems from multipath propagation environment where multiple copies of the transmitted signal are received at the receiver with different delays, amplitudes and phases. During demodulation period T_u, there will be overlap with other symbols of a different paths causing inter-symbol interference (ISI) and loss of orthogonality between subcarriers known as inter-carrier interference (ICI). Figure 6, shows ISI in multipath propagation environment where two paths are shown as an example, the direct component and delayed one.

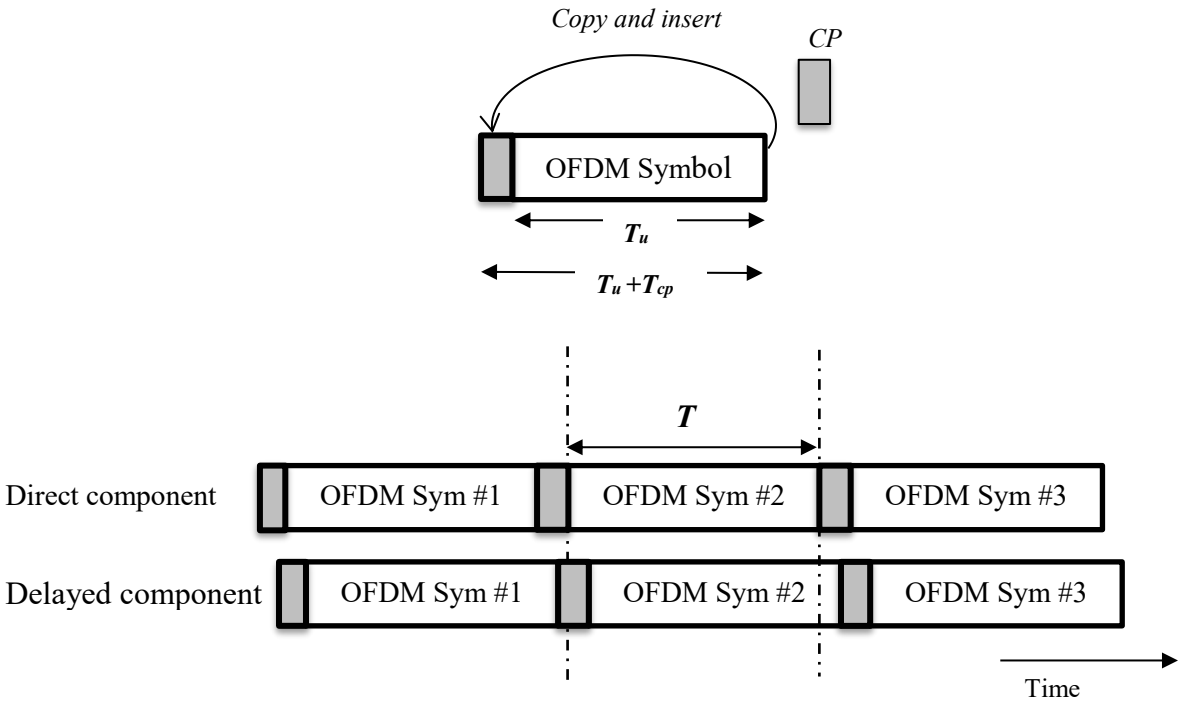

Figure 7. *ISI elimination by CP insertion*

ISI and ICI can be effectively eliminated by insertion of the so called cyclic prefix (CP). This can be done by copying the last part of OFDM symbol and insert it at the beginning of the OFDM symbol. CP insertion means that OFDM symbol length is increased to be *Tu+Tcp* , where *Tcp* is length of CP. Consequently, it increases the relative overhead. Figure 7, illustrates the insertion of cyclic prefix and its effect on multi-path propagation. It can be seen that ISI is eliminated, and orthogonality is maintained between subcarriers as long as *Tcp* is higher than the time span of the time dispersion of the radio channel.

Practically, CP is implemented as follows. The last N_{cp} samples of the IFFT output block of length N are copied and inserted at the beginning of the block. At the receiver side, the received signal is sampled at sampling rate f_s to get the sampled version r_n of the received signal. N_{cp} samples are removed before FFT processing block [8]. Baseband model of OFDM transmission and reception is given in Figure 8.

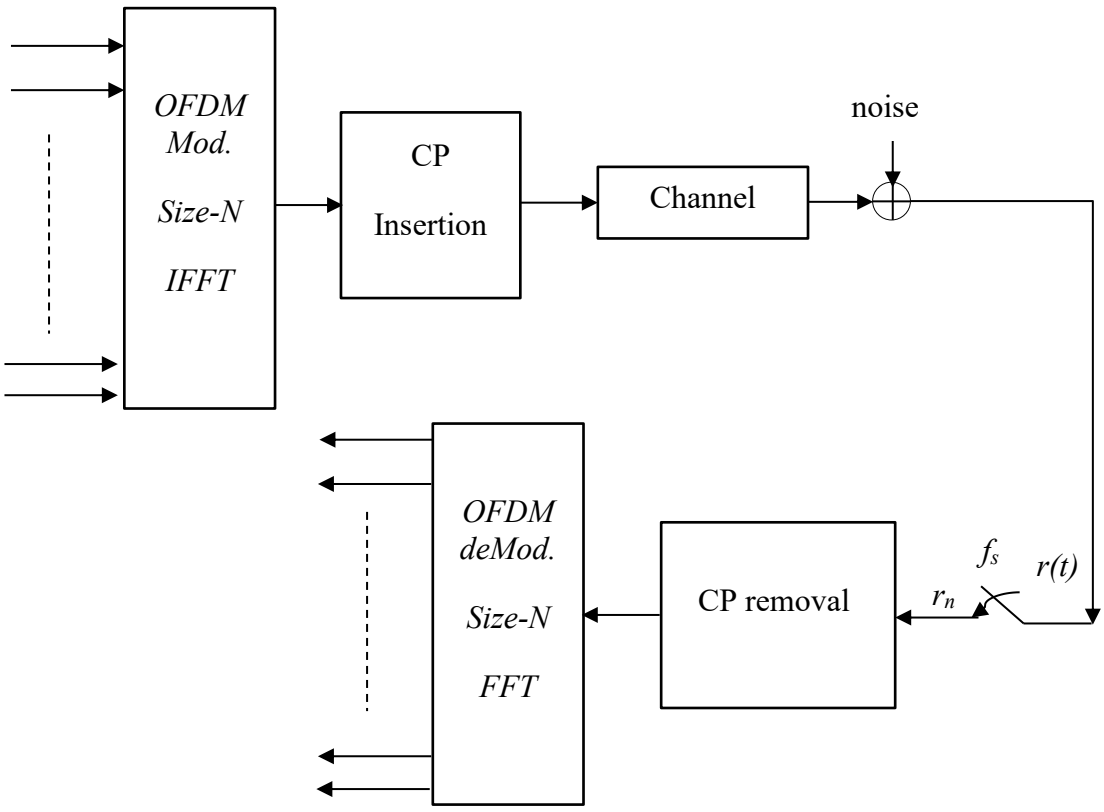

Figure 8. *Baseband model of OFDM transmission and reception*

It is worth noting that CP insertion effectively solves the ISI and ICI problem, but it comes with the price of increased signal overhead where redundant bits are transmitted resulting in reduced OFDM symbol rate. In general, there is a tradeoff between CP overhead and the ISI due to time dispersion that is not covered by the CP.

In 5G NR and unlike in LTE, flexible numerology with multiple subcarrier spacings are introduced to support diverse frequency bands, different deployment scenarios and use cases. 5G NR will operate in mmWave bands, where high bandwidth is being used (e.g., 100 MHz). In LTE, increasing bandwidth can be achieved by increasing the number of subcarriers which means increasing FFT size. This leads to increase computational complexity. In NR this can be avoided by using higher subcarrier spacing that allows for lower FFT size [4]. Also, a small subcarrier can support relatively long CP with reasonable overhead, whereas higher subcarrier spacing are more robust against phase noise with higher carrier frequencies expected to be used in NR [3]. Maximum component carrier bandwidth is 400 MHz can be supported. In case of larger bandwidth required, carrier aggregation can be used up to 16 component carriers, with maximum of 3300 active subcarriers per carrier component. Table 1, shows OFDM subcarrier spacings supported and maximum allowable bandwidth, where μ is given by higher layers configurations [10].

Table 1. *Supported transmission numerologies.*

μ	$\Delta f = 2^{\mu}.15\ kHz$	Max BW(MHz)	Cyclic prefix
0	15	50	Normal
1	30	100	Normal
2	60	200	Normal, Extended
3	120	400	Normal
4	240	-	Normal

2.2 DFT - Spread OFDM

Peak to average power ratio (PAPR) is the main drawback of the OFDM signal. PAPR problem reduces power amplifier efficiency significantly, especially in mobile terminals where the power amplifier design becomes more challenging and costly [13]. DFT-Spread OFDM is the transmission scheme used in 5G NR uplink data transmission for its desired properties that combine low PAPR, low complexity and high quality equalization [8]. DFTS-OFDM basic transmitter is illustrated in Figure 9. A block based transmission is supported similar to OFDM, where a block of *M* modulated symbols is applied to *M*-size DFT. The output of the DFT is applied to *N*-size IDFT with $N > M$, where the unused input bins are set to zero. The output of IDFT in this case will have single carrier properties with low PAPR and bandwidth depends on *M*. A CP is added to each transmitted block, allowing for low complexity frequency domain equalization at the receiver.

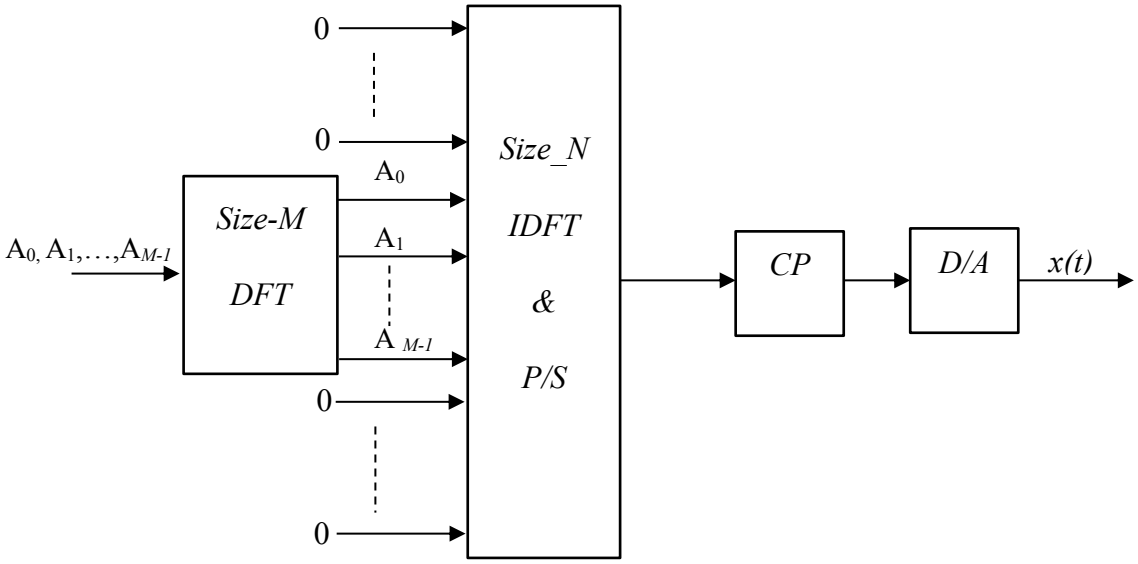

Figure 9. *DFTS-OFDM modulation.*

Flexible bandwidth assignment can be achieved by varying the block size *M,* where the transmitted bandwidth $BW = M/N \times f_s$, where *fs* is the sampling rate at the output of the IDFT. Moreover, user multiplexing can be achieved by controlling the DFT output mapping to IDFT input bins, so that the transmitted signal is shifted in frequency domain. DFTS-OFDM receiver structure is illustrated in Figure 10. Basically, the transmitter effect is being reversed. CP is removed for each received block. Then *N* size DFT operation is carried out. The output samples of DFT operation correspond to samples set to zero at the transmitter are discarded. For the radio channel frequency selectivity to be compensated, a frequency domain equalizer is applied after DFT block. Finally, *M* size IDFT is applied to the output of equalizer [17].

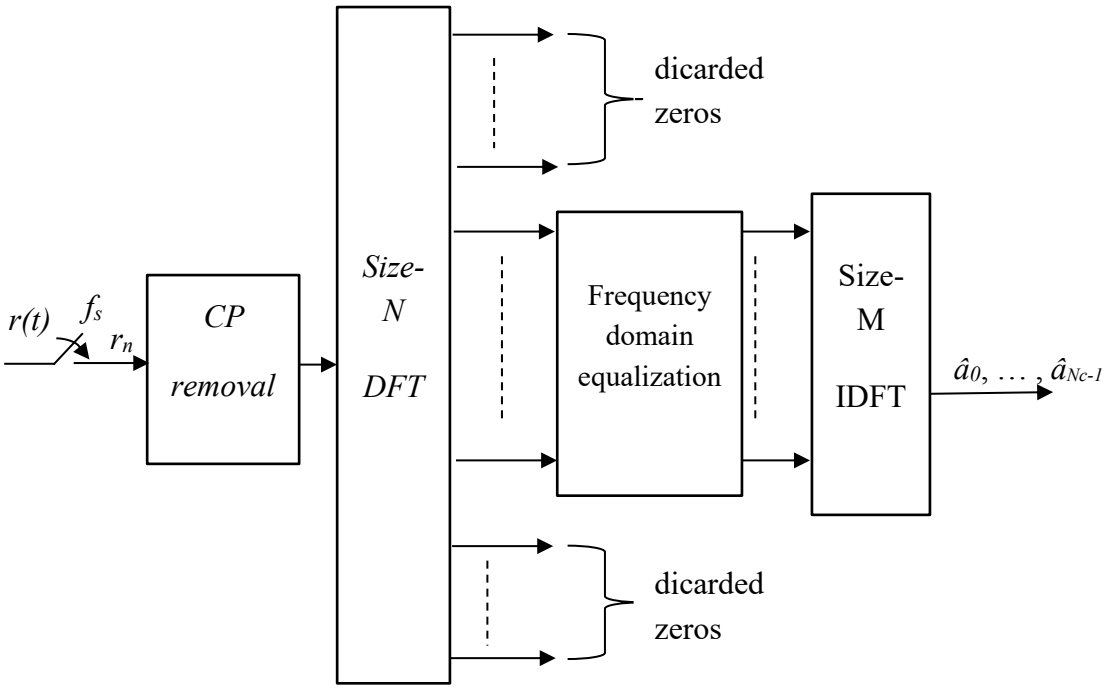

Figure 10. *DFTS-OFDM demodulation.*

2.3 Frame structure

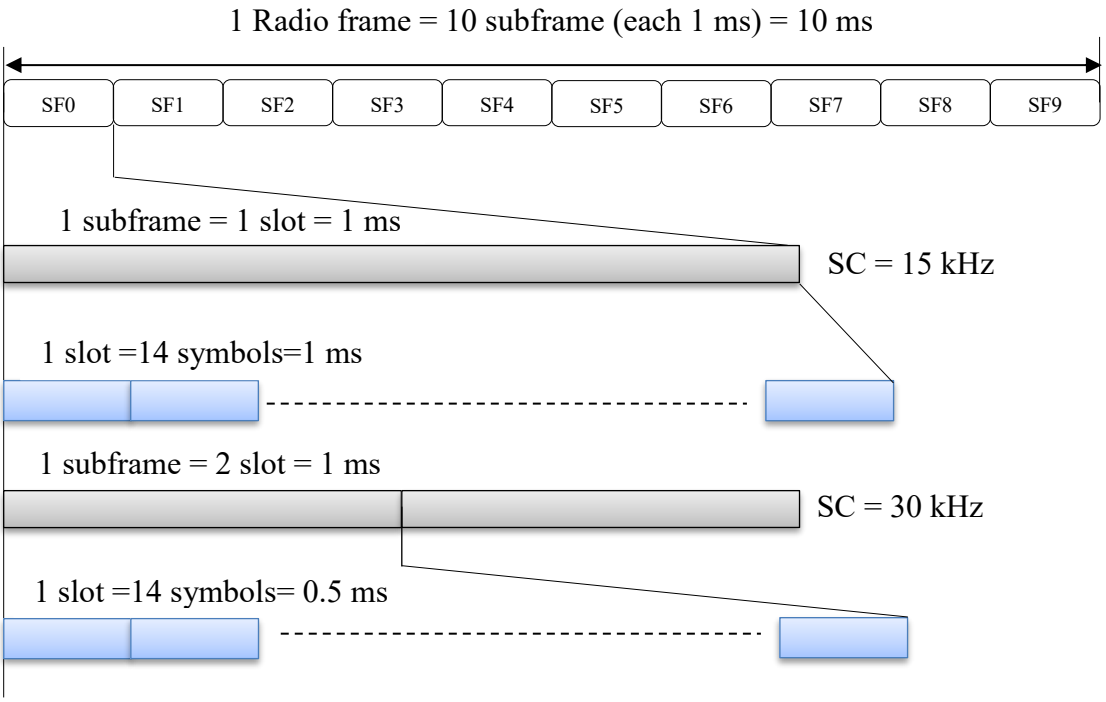

Figure 11. *5G NR frame structure for SC = 15, 30 kHz*

In the time domain, 5G NR transmissions are organized into frames of fixed length 10 ms, each frame is divided into an equally sized subframes of length 1 ms regardless the used subcarrier spacing numerology. Figure 11, shows the frame structure for μ= 0 and 1. It shows that for 15 kHz subcarrier spacing one subframe consists of one slot, while for 30 kHz subcarrier spacing one subframe consists of two slots. It should be noted that different numerology corresponds to different number of slots per subframe where number of OFDM symbols within subframe is fixed to 14 OFDM symbols. Table 2 shows that slot duration decreases as subcarrier spacing increase [10].

Similar to LTE, 5G NR available physical resources can be seen as a resource grid, where the subcarrier spacing defines the frequency step and the time dimension consist of consecutive OFDM symbols. A resource element (RE) is the smallest physical resource. It consists of one subcarrier during one OFDM symbol period and it can carry one complex valued symbol. REs are grouped into resource blocks (RB) each of which consist of 12 consecutive subcarriers in frequency direction and 14 OFDM symbols in time direction in case of normal CP (12 OFDM symbols in case of extended CP). The 5G NR physical resource grid is illustrated in Figure 12.

Table 2. *Slot length per numerology*

μ	$N_{\text{symb}}^{\text{slot}}$	$N_{\text{slot}}^{\text{frame},\mu}$	$N_{\text{slot}}^{\text{subframe},\mu}$
0	14 (1 ms)	10	1
1	14 (500 us)	20	2
2	14 (250 us)	40	4
3	14 (125 us)	80	8
4	14 (62.5 us)	160	16
5	14 (31.25 us)	320	32

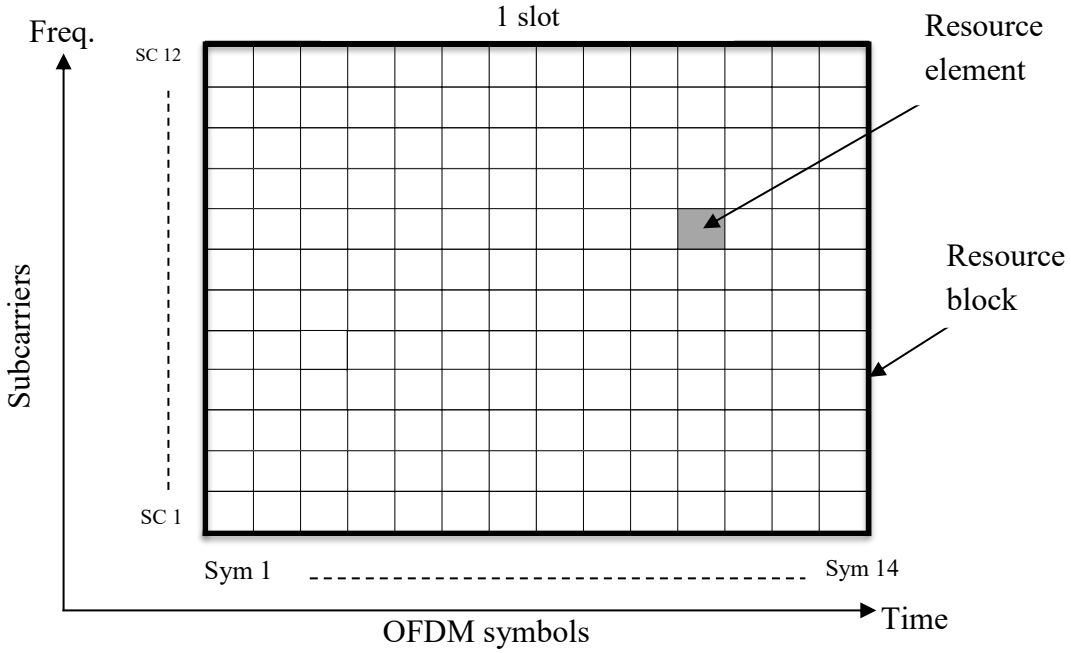

Figure 12. *5G NR time-frequency resource grid*

2.4 Reference signals

Reference signals are known symbols for both transmitter and receiver scheduled on specific resource elements in the time-frequency grid. In 5G NR different reference signals are introduced to support different functions. Demodulation reference signal (DM-RS) is mainly used by UE to estimate channel coefficients for coherent data modulation. Moreover, it can be also used for time and frequency offset estimation in the receiver. Phase-tracking reference signal (PTRS) is defined in NR to enable compensation of oscillator phase noise as it increases when operating in higher frequency bands (e.g. mmWave). Channel state information reference signal (CSI-RS) is introduced mainly to support CSI reports by UE, but it can be used in RRM measurements and other receiver algorithms.

5G NR has ultra-lean design principle that aims to minimize always-on transmissions, to enable higher network energy performance and enhance achievable data rates [3]. Always-on signals refer to signals transmitted for base station detection, system information broadcast and reference signals for channel estimation. Cell-specific reference signals (CRS) is an example for signals used for channel estimation for coherent demodulation. In LTE, different multi-antenna transmission schemes are mapped to different transmission modes (TM). These TMs are different in terms of structure of antenna mapping and what reference signals are used for demodulation process. There are ten different transmission modes defined. Single antenna transmission corresponds to TM 1 while, others correspond to multiantenna transmission schemes. CRS is used in transmission modes from 1 to 6 using antenna ports from 0 to 3 for demodulation of all physical channels, CSI reports and other receiver algorithms. DM-RS is used for transmission modes from 7 to 10 for data demodulation while CSI-RS is used of CSI reports. It should be noted that CRS is still present for other channels demodulation (e.g. PBCH and PDCCH) and for legacy UEs that not supports TMs 7 to 10. Unlike in LTE, 5G NR does not support cell-specific reference signals and NR reference signals are only transmitted when necessary. For example, DM-RS for data demodulation is only transmitted when there is data to be transmitted [8].

Downlink reference signals supported by NR are discussed next:

1- **Demodulation Reference Signals**

   DM-RS is UE-specific reference signal used by UE to estimate the radio channel coefficients for coherent data demodulation. It is only transmitted within the resource blocks assigned for transmission to that UE. DM-RS can support multiple layer MIMO transmission by scheduling multiple orthogonal DMRS ports, one for each layer. Orthogonality is achieved by FDM (comb structure), TDM and CDM (with cyclic shift of the base sequence or orthogonal cover codes) [14].

DM-RS density within resource block depends heavily on the channel properties, that if the channel is highly selective in frequency domain (i.e. smaller coherence bandwidth), higher density DM-RS allocation in frequency domain is adopted. Similarly, if the channel is more variant in time (i.e. smaller coherence time), more OFDM symbols are allocated for DM-RS. The front-loaded DMRS is basic pattern, as it enables early decoding requirement to support low-latency applications. DM-RS is allocated between control region and data region as illustrated in Figure 13, so when channel estimation is obtained using DMRS symbols, the data can be demodulated immediately.

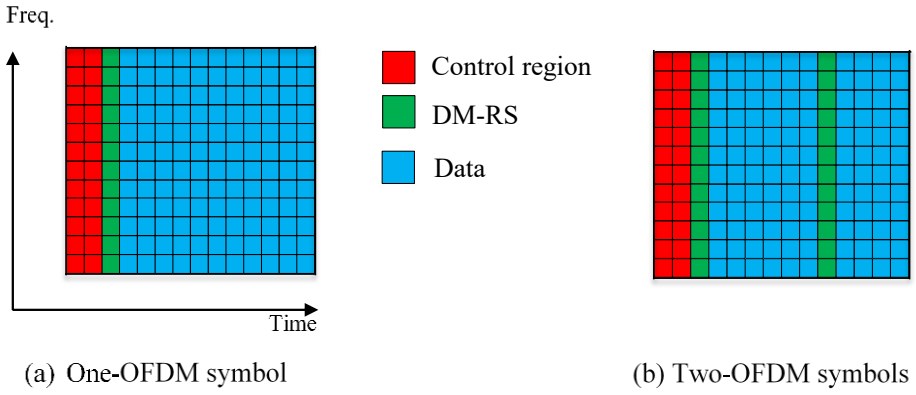

Figure 13. *Front-loaded DM-RS slot structure*

The front-loaded DM-RS pattern with one OFDM symbol allocation as illustrated in Figure 13a, is intended for low mobility cases where the channel coherence time is higher than slot duration. However, in higher mobility cases where coherence time is smaller than slot duration, one OFDM symbol is not enough to capture channel variations and channel estimation performance is degraded. So, two or more OFDM symbols can be allocated for DM-RS to capture channel variations in time. Figure 13b shows two OFDM symbols allocated for DM-RS. It should be noted that DM-RS symbols don't carry any useful data, so it is considered as overhead, so there is a tradeoff between channel estimation accuracy and DM-RS overhead [25].

2- Channel state information reference signals

CSI reference signal (CSI-RS) is first introduced in LTE Release 10. The main purpose for CSI-RS is to have separate reference signal to get CSI by UE. CSI reports are used by the base station for channel dependent scheduling, link adaptation and transmission settings of multi-antenna transmission. It should be noted that, higher degree of flexibility and more optimization can be achieved by having separate reference signals for channel estimation and to get channel state infor-

mation. DM-RS is transmitted with high density only when there is data transmission. CSI-RS is an efficient tool to get CSI for given number of network nodes and antenna ports.

The structure of the CSI-RS used by UE is given by the higher layer parameter *NZP-CSI-RS-Resource configuration.* CSI-RS is transmitted on 1, 2, 4, 8, 12, 16, 24 or 32 antenna ports. In time domain, CSI-RS can be scheduled with different periodicity starting from 5 ms up to 640 ms, in other words it can be scheduled twice every frame up to every 64 frames. CSI-RS periodicity and the exact subframe in which CSI-RS is scheduled can be also configured by *CSI-RS time configuration* as part from higher layer parameter mentioned above [26].

Zero-Power CSI-RS

ZP CSI-RS can be defined as a set of resource elements with the same structure as conventional Non-Zero Power CSI-RS. The idea with Zero-Power CSI-RS is to define additional resources which UE should assume that PDSCH is not mapped. These resources may be used for interference measurements colliding with CSI-RS corresponding to another interfering links. Moreover, it may correspond to CSI-IM resources discussed later in section 3.5 [8].

3- Phase-tracking reference signals (PTRS)

PTRS is introduced in NR to enable compensation of oscillator phase noise. Typically, phase noise increases as a function of oscillator carrier frequency. PTRS can therefore be utilized at high carrier frequencies (such as mmWave) to mitigate phase noise. One of the main degradations caused by phase noise in OFDM signal is identical phase rotation of all the subcarriers, known as common phase error (CPE). PTRS is designed so that it has low density in frequency domain and high density in time domain, since the phase rotation produced by CPE is identical for all subcarriers within an OFDM symbol, but there is low correlation of phase noise across OFDM symbols. PTRS is UE-specific, confined in a scheduled resource and can be beamformed. The number of PTRS ports can be lower than the total number of ports, and orthogonality between PTRS ports is achieved by means of FDM. PTRS is configurable depending on the quality of the oscillators, carrier frequency, OFDM subcarrier spacing, and modulation and coding schemes used for transmission [14].

2.5 Channel coding

5G NR channel coding is based on low-density parity check (LDPC) codes for the data channel. LDPC codes are defined by their parity check matrices, with each column representing a coded bit, and each row representing a parity check equation. LDPC decoding is done by exchanging messages between variables and parity checks in an iterative manner. The LDPC codes proposed for NR use a quasi-cyclic structure, where the parity check matrix is defined by a smaller base matrix. Similar to LTE, hybrid automatic repeat request (HARQ) retransmission using incremental redundancy is supported, where the erroneous received data can be retransmitted by the gNodeB and the UE combines the soft information from multiple transmission attempts.

Polar codes will be used for layer1 and layer2 control signaling, except for very short messages. It will be also used for channel coding for broadcast channel. Polar codes are the first class of codes shown to achieve the Shannon capacity with reasonable decoding complexity for a wide variety of channels. By concatenating the polar code with an outer code and keeping track of the most likely values of previously decoded bits at the decoder (the list), good performance is achieved at shorter block lengths, like those typically used for layer 1 and layer 2 control signaling. By using a larger list size, error correction performance improves, at the cost of higher complexity at the decoder [14].

2.6 Physical channels

In this section, a brief introduction of physical channels is introduced. In general, physical layer is responsible for layer-1 physical channels, generation of physical signals and modulation. It defines the uplink and downlink physical channels, frame structure, data modulation (e.g. BPSK, QPSK, etc.) and physical resources mapping. Moreover, OFDM signal generation and multi-antenna processing.

Basically, a physical channel is mapped to set of resource elements carrying information generated from higher layers. 5G NR defines in total six physical channels. In downlink transmission three physical channels are defined as physical downlink shared channel (PDSCH), physical broadcast channel (PBCH) and physical downlink control channel (PDCCH). Similarly, in uplink transmission three physical channels are defined: physical uplink shared channel (PUSCH), physical uplink control channel (PUCCH) and physical random-access channel (PRACH). PDSCH and PUSCH are the main physical channels that carry the user data to/from user equipment. The term “shared” stems from the fact that, there are simultaneous frequency separated transmissions to different UEs. In order for the UE/base station to receive and decode the transmitted data, there are other physical channels introduced to provide the necessary control information. For example, PBCH carries system information for the UEs to access the network. PDCCH plays a key role in

downlink transmission as it carries scheduling information that defines downlink scheduled resources, uplink power control instructions, uplink resource grants and transmission scheme and MCS [8].

2.7 5G NR spectrum and Duplex schemes

As mentioned earlier, 5G NR will support multiple and diverse use cases and deployment scenarios. This will require different bandwidths to support different deployments. For example, mMTC will require relatively small bandwidth. In contrast, for eMBB very high data rates are supported that requires very large bandwidth. In 3GPP Release 15 the first 5G NR standard, a wide range of operating bands are supported up to 52.6 GHz. These bands are categorized into two frequency ranges: Sub 6 GHz range is called frequency range one (FR1) and frequency range two (FR2) also known as millimeter wave band (mmWave) [15]. Table 3, defines the corresponding frequency allocations for each frequency range.

Table 3. *NR frequency ranges*

Frequency ranges	Spectrum allocation
FR1	450 MHz - 6000 MHz
FR2	24250 MHz – 52600 MHz

Most of nowadays commercial radio communications such as AM/FM radio, cellular systems and satellite communication are operating in a small part of RF spectrum that is 300MHz to 3GHz. This band has desirable propagation characteristics that attracts these services. However, due to increase demand for higher data rates and system capacity, frequency bands higher than 3 GHz need to be exploited. Spectrum range between 3-300 GHz defines mmWave frequency band that corresponds to wavelengths from 1 to 100mm. It allows for very large system bandwidth that enables eMBB applications. Propagation characteristics of mmWaves band are challenging. For example, high free space path loss that accounts for most of signal losses due to high carrier frequency. This problem can be solved by means of beamforming techniques. Moreover, mmWaves suffer from very high penetration losses as it can't penetrate most of solid material. Heavy rains can cause significant signal losses. Raindrops are nearly same size of the signal wavelength causing scattering of propagating signal [7].

5G NR will support both FDD and TDD duplexing schemes. The first 5G NR standard Release 15, will focus on dynamic TDD. In dynamic TDD, each OFDM symbol in a slot can be allocated as downlink, uplink or flexible based on the scheduler decision.

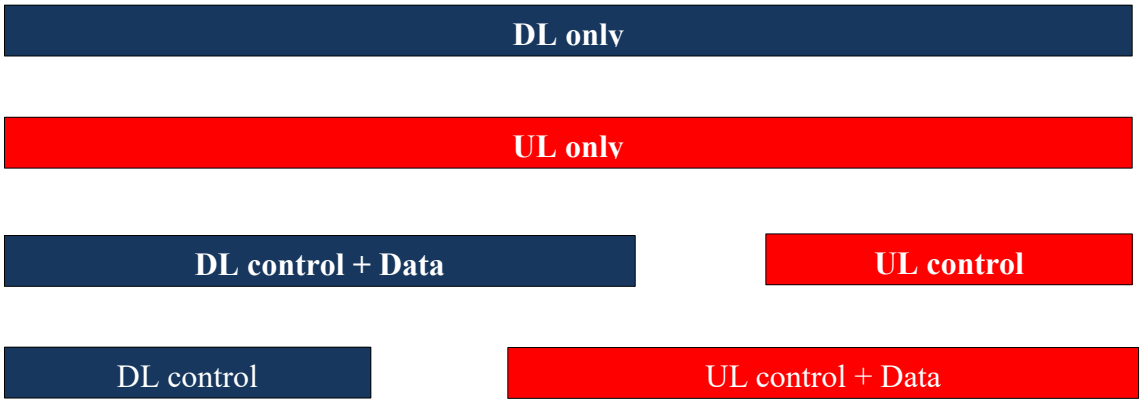

Figure 14. *Slot format configurations*

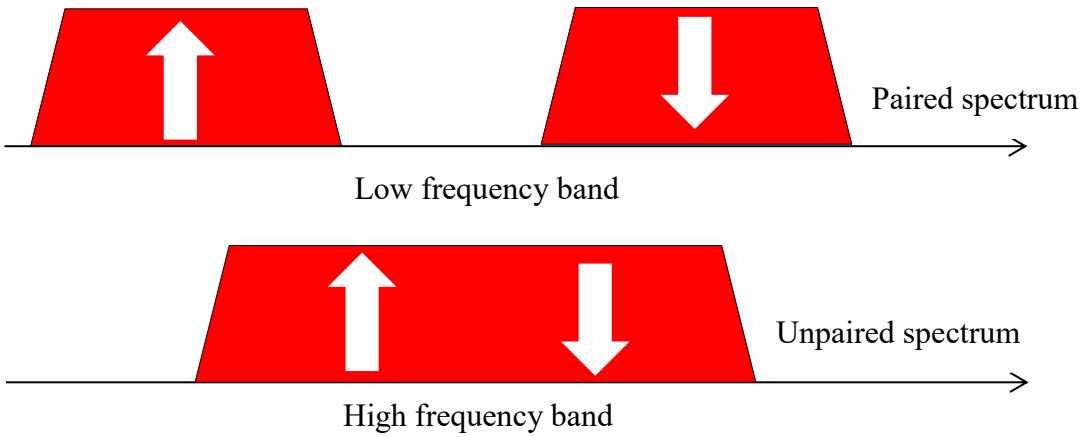

Figure 15. *Paired and unpaired spectrum allocations*

As can be seen from Figure 14, slot can be scheduled to be only downlink transmission, only uplink transmission or the newly introduced concept of self-contained slot to support low latency requirements applications and allows multiplexing of different services in the same network. Slot format is defined according to Table 4.3.2-3 in [10] which contains 62 different slot formats and up to 255 reserved for future use.

Both paired and unpaired spectrum are supported in 5G NR. Figure 15, shows that at lower frequency bands, allocations are paired with FDD operation. Unpaired spectrum is used at high frequency bands allowing TDD operation [12].

2.8 Multi-antenna transmission and Beamforming

5G NR will be using different multi-antenna technologies based on the operating frequency band. In general, a massive number of controllable antenna elements will be deployed in the base station allowing simultaneous transmission and reception with multiple spatially separated users. At lower frequency bands, full-dimension MIMO is enabled with antenna elements up to 32 and FDD operation is supported. This needs channel knowledge at the base station, hence CSI-RS is transmitted in the downlink transmission and CSI reports are delivered in the uplink direction. Transmission with high bandwidth is not available in this band so high spectral efficiency is achieved by higher order spatial multiplexing. At higher frequency bands, a larger number of antenna elements can be adopted in a given area due to shorter wavelengths which enhances the performance of beamforming and MU-MIMO. TDD operation is assumed and channel reciprocity is exploited where high resolution CSI is required at the base station. Uplink reference signals are used to estimate the channel response in the uplink direction. The CSI is then used in uplink "receive combining" and downlink "transmit precoding". For higher frequency bands i.e. mmWave band, a very large number of antenna elements is used for beamforming to maintain coverage and overcome the increased path loss [14].

3. THEORETICAL FRAMEWORK AND FUNDAMENTALS

In this chapter, thesis theoretical framework is introduced. The concept of link level simulator and the proposed interference model are explained. Then radio communication channel is discussed briefly. Moreover, basic understanding of LA is discussed since its performance is directly related to the quality of interference measurement. LA is an essential part of any cellular system and it is used by base station to adapt the transmission settings based on interference and channel conditions at UE. CSI feedback in the form of CQI gives base station recommendation about the next transmission parameters. CSI reports is prepared based on channel and interference measurements in the UE. The concept of CSI feedback and related channel and interference measurements are explained in detail in this chapter.

3.1 Link level simulator and interference model

Performance of wireless communication systems can be measured in two levels known as: link-level and system-level simulations. Link-level simulation usually measures the performance of different physical layer technologies where single cell and single UE is typically simulated. In link-level simulations the transmitter is modeled, so the transmitted signal is generated and then distorted by modeling the channel effect. Receiver side is also modeled where AWGN is added to the received signal then different receiver algorithms are applied to recover the transmitted signal. There are different performance metrics used in link-level simulations, for example: link throughput (TP) and block error rate (BLER) against link signal to noise ratio (SNR) or signal to interference plus noise ratio (SINR). On the other hand, System-level simulations are essential to evaluate network performance in different load scenarios and in network planning. In this thesis, link level simulator is extended to support multi-cell scenario. It has capability to simulate 5G NR downlink transmission and it is used to evaluate the cell-edge user performance with the given interference model.

The proposed interference model consists of one serving gNB and two interfering gNBs as shown in Figure 16. In order to reduce complexity, only the closest two interferers are modeled and the other distant interferes are assumed to be additional noise. The simulator generates independent downlink data transmissions from interfering gNBs that are distorted by the radio channel and added to the useful data transmission received from the serving gNB with interference to noise ratio (INR) profile adopted.

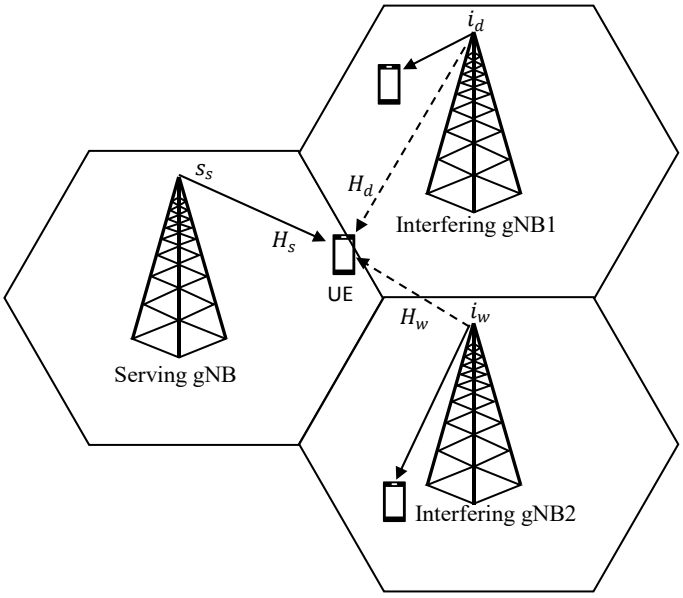

Figure 16. *Interference model consists of one serving cell and two interfering cells*

In Figure 16, $\mathbf{s}_s$, $\mathbf{i}_d$, and $\mathbf{i}_w$, are the received signals by the intended UE from serving cell, dominant interferer cell and weaker interferer cell respectively, and $\mathbf{H}_s$, $\mathbf{H}_d$, and $\mathbf{H}_w$ represents the channel responses of the received signals. Many companies have evaluated different INR profiles and interference settings are agreed by 3GPP for the companies to simulate with the same settings [23]. INR profiles can be mapped to the so called Dominant Interferer Proportion (DIP) profiles, which are used in the simulator. INR profiles defines the SNR of the explicitly modeled interferes(s) whereas, DIP profile defines power ratio(s) between the explicitly modeled interferer(s) and the overall interference plus noise power. In this thesis INR3 is used for simulations that maps to DIP profile of [-0.524416 -11.09441] dB. The exact mapping between INR profile to DIP profile is not in the scope of this thesis.

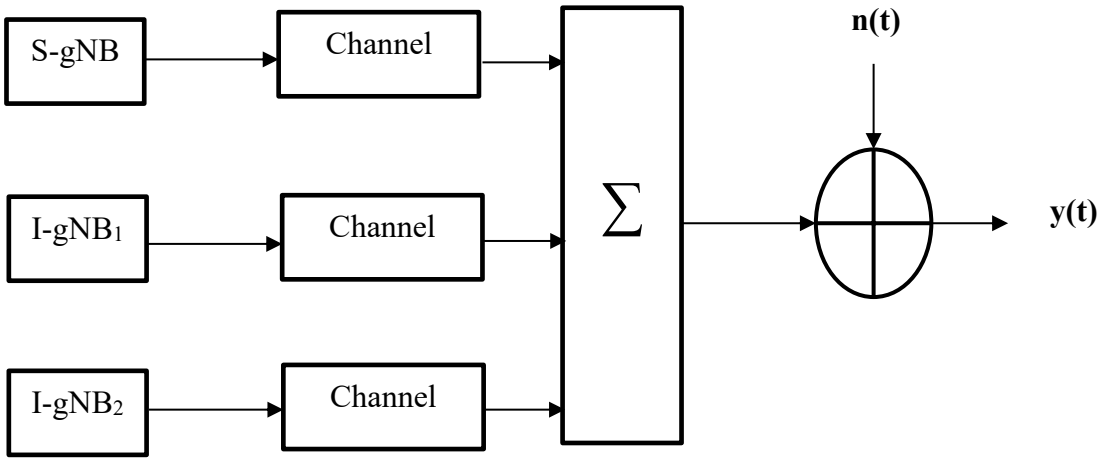

Figure 17. *Extended link-level simulation*

Extended link-level simulation with multi-cell scenario can be seen in Figure 17. Where S-gNB represents the serving gNB transmitting useful data, I-gNB represents interfering gNBs transmitting interfering signals and *n(t)* represents AWGN noise component. Each signal is generated and distorted independently by the radio channel. Figure 17, shows that useful signal is distorted by noise and signals from interfering gNBs. The overall received signal can be represented as follows:

$$\mathbf{y}(t)_j = \sum_{i=0}^{N_t-1} \mathbf{x}_i(t) * \mathbf{h}_{ij}(t) + \mathbf{n}_\mathrm{j}(t) + \sum_{m=0}^{N_{cell}-1} \sum_{i=0}^{N_t-1} \mathbf{i}_{i,j}(m,t) \qquad (3.1)$$

where N_t represents the number of transmit antennas, N_{cell} represents the number of interfering gNBs. $I_{i,j}(m,t)$ represents interfering signal from interfering gNB m transmitted from antenna i to receive antenna j.

3.2 Radio communication channel

The radio communication channel is characterized by a very fast and random variations in channel conditions. These variations can be categorized into large-scale variations and small-scale variations. Large-scale variations are for example, path loss defined as the mean loss of signal strength for a given distance between transmitter and receiver. In addition to path loss, there is shadow fading due to large obstacles in the signal path. Multipath propagation environment results in small scale variations defined as very fast fluctuations of the received signal level over very short distance or time. Small scale variations results in frequency selectivity of the radio channel.

In multipath propagation environment, multiple copies of transmitted signal reach receiver with different delays and powers. These copies are combined at the receiver and can be added constructively or destructively. If the received copies are arrived with very small delays compared to symbol duration, the radio channel is considered to be flat or non-frequency selective. However, if the symbol duration is small for example in wideband transmissions, the received signal delays are high compared to the symbol duration resulting in frequency selective fading. On the other hand, radio channel time selectivity is directly related to receiver mobility and can be characterized by coherence time. Coherence time defines how long the channel condition remains constant with a certain correlation. It measures how fast the channel changes, so slowly changing channel has high coherence time and vice versa [24].

3.3 Link adaptation

Link adaptation (LA) is a key feature that is used in every mobile communication cellular system. It refers to adapting transmission settings to take advantage of the varying channel response. The transmission settings to be adjusted are for example: modulation order and coding rate known as rate adaptation. Transmission power can be also adjusted known as link adaptation by power control. The purpose of LA is to improve system capacity, peak data rates and coverage reliability. System capacity is improved by efficient utilization of frequency spectrum as it is very scarce and expensive resource in wireless communications [21]. In principle, LA aims to exploit the varying nature of the radio channel by dynamically changing the transmission settings based on the changing channel conditions and interference levels at the UE. LA is performed at the base station and decisions about the next transmission settings (e.g. modulation order and code rate) are based on CSI reports provided by the UE. CSI reports to be explained next in Section 3.4.

In practice, the values of transmission settings are grouped and quantized together in so called modulation and coding schemes (MCS). In 5G NR two different MCS tables are defined in [26]. Table 4, shows the first table consists of 29 indices, corresponds to QPSK up to 64 QAM modulation scheme. Second table consists of 28 indices corresponds to QPSK up to 256 QAM. Each index of these table is a combination of modulation order, target code rate and the corresponding spectral efficiency. Since each index of these tables has different data rates and robustness level i.e., minimum SNR needed to activate the corresponding MCS. They are optimal to be used in different channel/link quality regions. The goal of LA is to ensure that the most efficient MCS is always used over varying channel conditions. Very low MCSs are used to enable communications in poor channel conditions which makes the system robust. On the other hand, when the channel conditions are high, spectrally efficient MCSs are used to increase throughput. So, the key to successful LA is the availability of accurate CQI at the base station which provides the channel knowledge to choose the most efficient MCS. In contrast, systems that don't enable LA chooses fixed MCS to maintain a certain level of throughput when the channel conditions are poor.

Table 4. *MCS table up to 64 QAM.*

MCS Index	Modulation Order	Target code Rate × 1024	Spectral efficiency
0	2	120	0.2344
1	2	157	0.3066
2	2	193	0.3770
3	2	251	0.4902
4	2	308	0.6016
5	2	379	0.7402
6	2	449	0.8770
7	2	526	1.0273
8	2	602	1.1758
9	2	679	1.3262
10	4	340	1.3281
11	4	378	1.4766
12	4	434	1.6953
13	4	490	1.9141
14	4	553	2.1602
15	4	616	2.4063
16	4	658	2.5703
17	6	438	2.5664
18	6	466	2.7305
19	6	517	3.0293
20	6	567	3.3223
21	6	616	3.6094
22	6	666	3.9023
23	6	719	4.2129
24	6	772	4.5234
25	6	822	4.8164
26	6	873	5.1152
27	6	910	5.3320
28	6	948	5.5547
29	2	reserved	
30	4	reserved	
31	6	reserved	

The capacity improvement offered by LA over non-adaptive systems can be remarkable as seen in Figure 18. In this figure we present link level spectral efficiency (SE) performance (bits/s/Hz) vs. signal to noise ratio (SNR). For simplicity only three different MCSs are used, for example: MCS 1 (QPSK, code rate = 0.1533), MCS 10 (16 QAM, code rate = 0.3320) and MCS 20 (64 QAM, code rate = 0.5537). The first system is non-adaptive with MCS index 1 (red curve). In the second system, LA is enabled and it corresponds to the envelope of three MCS (green curve). It is clear that, each MCS is optimal to be used in different SNR range and LA chooses the MCS with the highest spectral efficiency in each SNR range. Spectral efficiency of two systems is equal up to SNR = 2

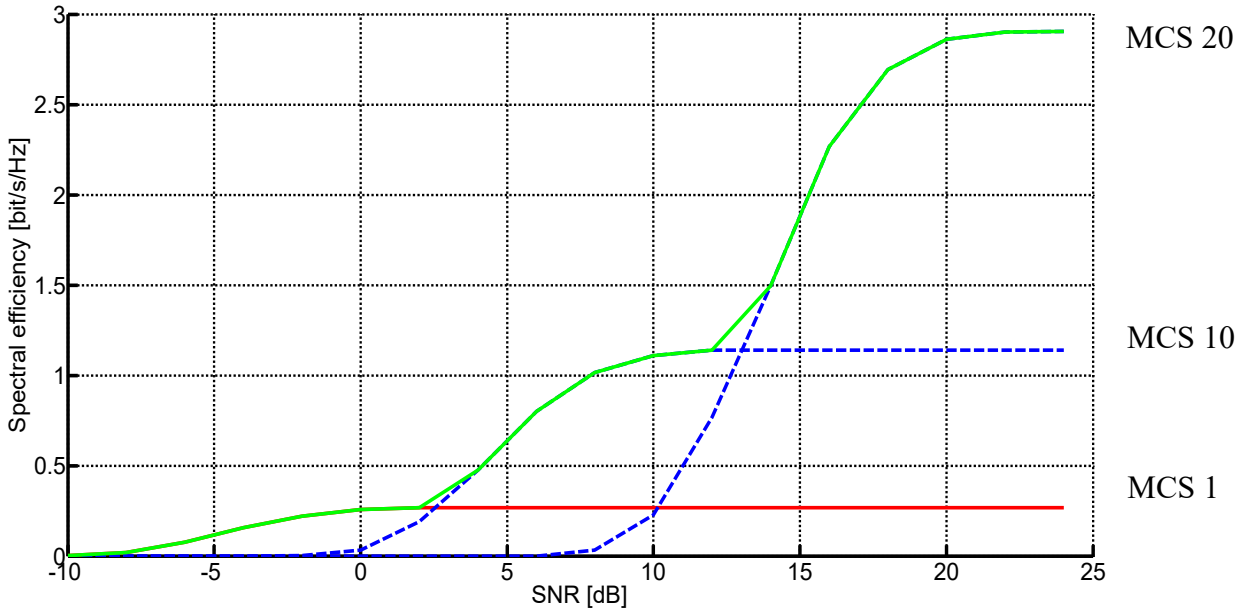

Figure 18. *Adaptive and non- adaptive systems spectral efficiency.*

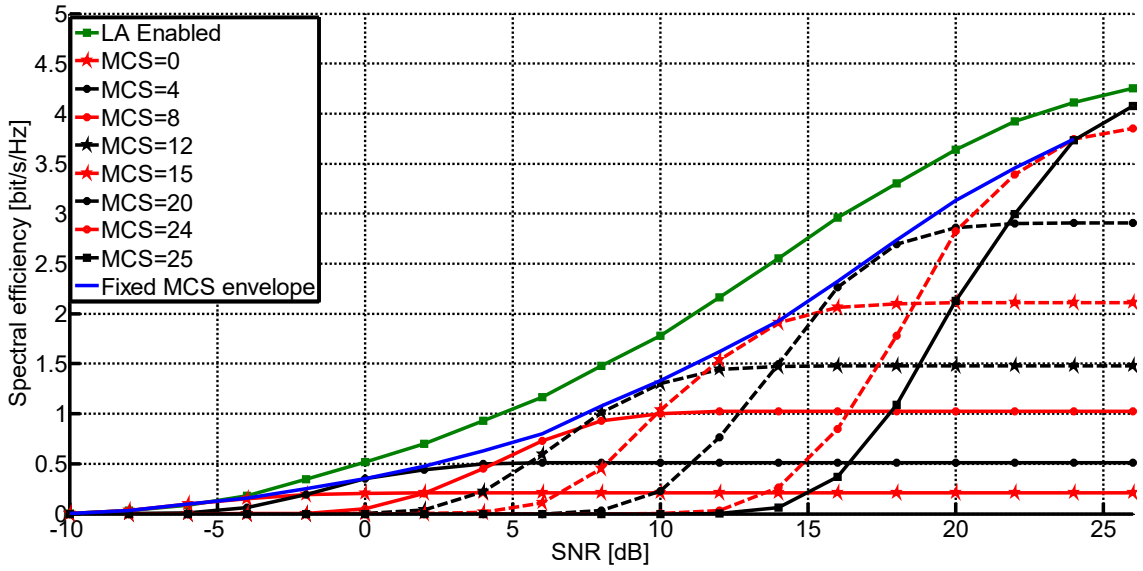

Figure 19. *Link adaptation spectral efficiency compared to fixed MCS envelope*

dB. However, in high SNR range the spectral efficiency of adaptive system is approximately 10 times higher than that of non- adaptive system. In Figure 18, fixed MCS curves were simulated under assumptions of single layer single antenna port, LDPC channel coding, 3GPP tdl-c-300 ns channel model, 15 kHz subcarrier separation, 50 PRB, ideal channel estimation and user speed of 3 kmph.

As discussed above LA exploits advantageous channel conditions to increase system spectral efficiency and overall delivered throughput. This can be seen from Figure 19, where the first system with LA enabled (green curve) is compared to non-adaptive system where an envelope of 28 MCS indices (only few are plotted) of Table 4 above is presented in blue curve. It is clear that the overall delivered throughput of the adaptive system is higher than non-adaptive system. This is because LA system chooses the most efficient MCS given the current channel condition based on available CQI report, i.e. the MCS that delivers the highest throughput. This process will be discussed in details in Section 3.8.

Outer loop link adaptation

Outer loop link adaptation (OLLA) is a process that aims to correct inaccuracies of CQI calculations so that a certain target block error rate (BLER) of the first HARQ transmission can be achieved. These inaccuracies are due to estimation errors in channel and interference measurements performed by UE. Moreover, there is a delay between CQI calculations and when it is available at the base station. Also, wideband CQI is reflecting the average channel conditions across the system bandwidth which introduces errors in reported CQI. OLLA is performed by the base station and different schemes are proposed in the literature to cope with inaccuracies of CQI calculations. In [27], a scheme that subtracts an adaptive offset (Δ_{OLLA}) from the reported signal quality based on the HARQ acknowledgments is proposed:

$$\mathrm{CQI} = \mathrm{CQI} - \Delta_{OLLA}\,[dB] \tag{3.2}$$

If the transmitted block is correctly decoded, then positive acknowledgement (ACK) is received and Δ_{OLLA} is decreased by Δ_{down}. If negative acknowledgement (NACK) is received, then Δ_{OLLA} increased by Δ_{up}. the values of Δ_{down} and Δ_{up} is related to the target BLER as follows:

$$BLER_{Traget} = \frac{1}{1+\frac{\Delta_{up}}{\Delta_{down}}} \tag{3.3}$$

It should be noted that, in this thesis OLLA is not enabled. Since the scope of this thesis is to find the optimal interference measurement scheme that results in overall best performance. So, correction of CQI inaccuracies is left out of the thesis scope.

3.4 Channel state information

Channel state information (CSI) provided by the UE to the base station enables downlink LA. CSI at the base station allows to choose transmission settings based on the channel conditions and interference levels at the UE.

CSI reports consist of channel quality indicator (CQI), precoding matrix index (PMI), CSI-RS resource indicator, layer indication(LI), rank indication (RI) and / or L1-RSRP. However, in this thesis we focus on channel quality indicator as one of the CSI components that reflects average channel conditions and interference levels at UE. CQI defines the highest modulation order and coding rate for downlink transmission to achieve target received block error rate (BLER) for example 10% with the recommended RI and PMI. Rank indication (RI) gives recommendation on the number of layers to be supported on downlink transmission to the UE. Precoder matrix indication (PMI) gives recommendation on the precoder to be used in downlink transmission. If the UE is in spatial multiplexing mode, then PMI and RI are reported otherwise they are not needed.

Channel and interference measurements are essential to prepare CSI reports. Channel gains can be obtained from CSI-RS. However, accurate interference measurement is challenging. In LTE release 11, CSI-interference measurement (CSI-IM) is defined, where a set of resource elements in one subframe are configured by the network on which the interference can be measured by the UE. Basically, CSI-IM has the same structure as CSI-RS with nothing transmitted in these resources by the gNB. Practically, ZP CSI-RS will cover CSI-IM resources, where the received power from interfering gNBs in these resources are used for interference plus noise measurement. It should be clear that, CSI-IM and ZP CSI-RS has different functions where CSI-IM defines the set of resource elements where interference level is measured, and ZP-CSI defines a set of resource elements where PDSCH is not mapped [8]. Figure 20, shows CSI signals allocations within one subframe. The number of REs per PRB is determined by higher layer parameters.

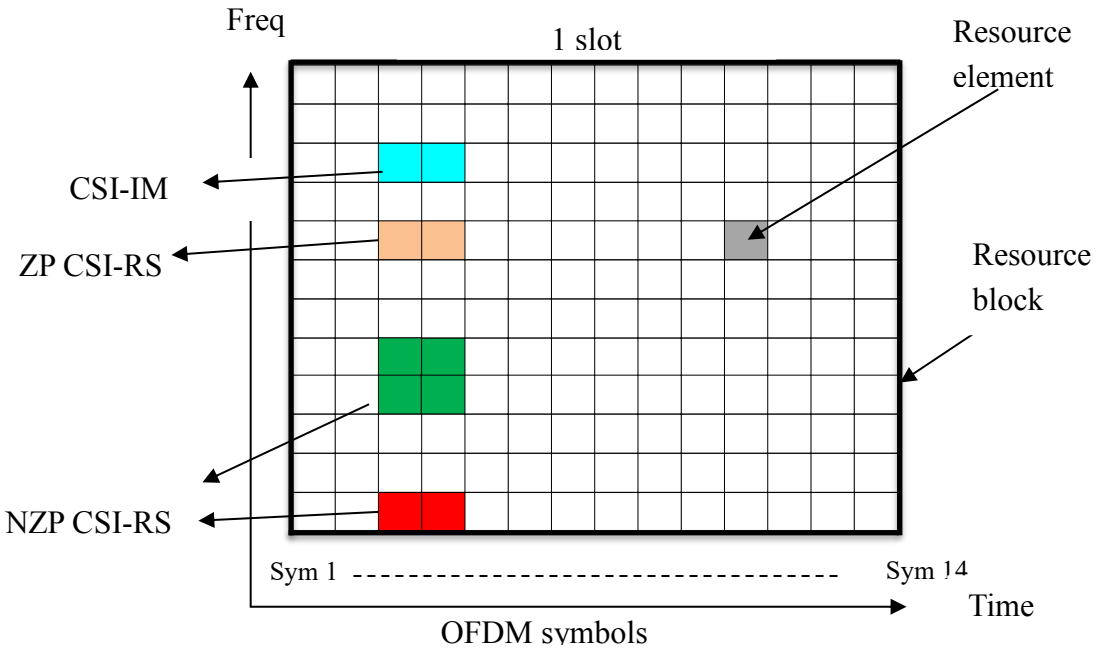

Figure 20. *CSI reference signals allocations within resource grid*

CSI reporting modes

In 5G NR UE can be configured to report CSI in aperiodic, periodic or semi-persistent reporting modes. Aperiodic CSI reports are carried out on PUSCH upon explicit request from the network. It has larger contents and details since it is carried out using PUSCH that allows for larger payload. Moreover, since it is only transmitted when needed, it has less overhead compared to periodic transmission. Periodic CSI reports are usually carried out on PUCCH or on PUSCH if UE has a valid uplink grant. It can be configured with different periodicities from 5 ms up to 640 ms. Periodic CSI reports has less information compared to Aperiodic reports since it is carried out using PUCCH that allows limited payload. Semi-persistent CSI reporting can be seen as a time windowed version of periodic CSI reporting. It is activated by downlink control indicator (DCI) and reported on PUSCH or PUCCH periodically until the semi-persistent CSI reporting is deactivated [26].

CSI reports can be configured with three different modes. It can be wideband reports, UE-selected reports and higher layer configured report. In wideband reports, a single CQI is reported that reflects the average channel condition through the entire cell bandwidth. This mode is supported in both periodic and aperiodic CSI reports. In UE-selected reports, the UE reports M CQIs that represent M preferred sub-bands. This mode is also supported in both periodic and aperiodic CSI reports. Higher layer configured reports are only supported in aperiodic CSI reports where one wideband CQI and one CQI per sub-band are reported [8]. It should be noted that in this thesis only periodic wideband reports are used in link level simulations.

3.5 Channel estimation

As discussed in Section 2.4, 5G NR uses two different reference signals for channel estimation, each of which is serving two different functions. DM-RS is used for coherent data demodulation and it is only transmitted whenever there is data to be transmitted. On the other hand, CSI-RS based channel estimation is used by UE to prepare CSI reports needed for downlink LA and only transmitted on a certain periodicity configured by gNB. Next, we discuss a common practical implementation for channel estimation based on Wiener filtering. In this implementation two cascaded one-dimension Wiener filters are used, where the first one is in frequency direction and the second is in time direction.

In general, channel estimation is carried out using known reference signals for both transmitter and receiver. Reference signals are scheduled in the time-frequency grid with reasonable density so that accurate channel estimation can be obtained. Typically, in frequency direction the spacing between reference symbols should be less than channel coherence bandwidth. Similarly, in time direction the separation between reference symbols should be less than channel coherence time. In practice, first channel is estimated on these positions where reference symbols are scheduled to get raw channel estimation.

Then there are several ways to get channel estimation between these reference symbols. Next a very common and practical interpolation approach based on 2 × 1-D Wiener filters are introduced.

Wiener filter concept

Wiener filter aims to minimize mean square value of estimation error, where estimation error can be expressed as:

$$\boldsymbol{\varepsilon} = \mathbf{h} - \hat{\mathbf{h}} \tag{3.4}$$

where **h** is the actual channel response and $\hat{\mathbf{h}}$ is the estimated channel response. The mean square error is in the form:

$$\mathbf{J} = E\{\|\boldsymbol{\varepsilon}\|^2\} \tag{3.5}$$

wiener filter generates continues channel estimates for all subcarriers, i.e. for subcarriers not carrying reference symbols using input raw channel estimates on the positions where reference symbols are located. In this thesis, channel estimation is carried out using two cascaded 1-D Wiener filters. The first filter is in frequency direction while the other is in time direction. However, the reversed order will result in the same performance due to filters linearity.

This implementation of 2 × 1-D Wiener filters are proposed since it has low complexity with satisfactory performance. Basically, the first 1-D Wiener filter in frequency direction takes raw channel estimates at REs carrying reference symbols as an input and interpolates the channel estimates to all REs not carrying reference symbol in frequency direction. The second stage is performing interpolation in time direction as illustrated in Figure 21. Next 2 × 1-D Wiener filters are explained in more details.

2 × 1-D Wiener filters

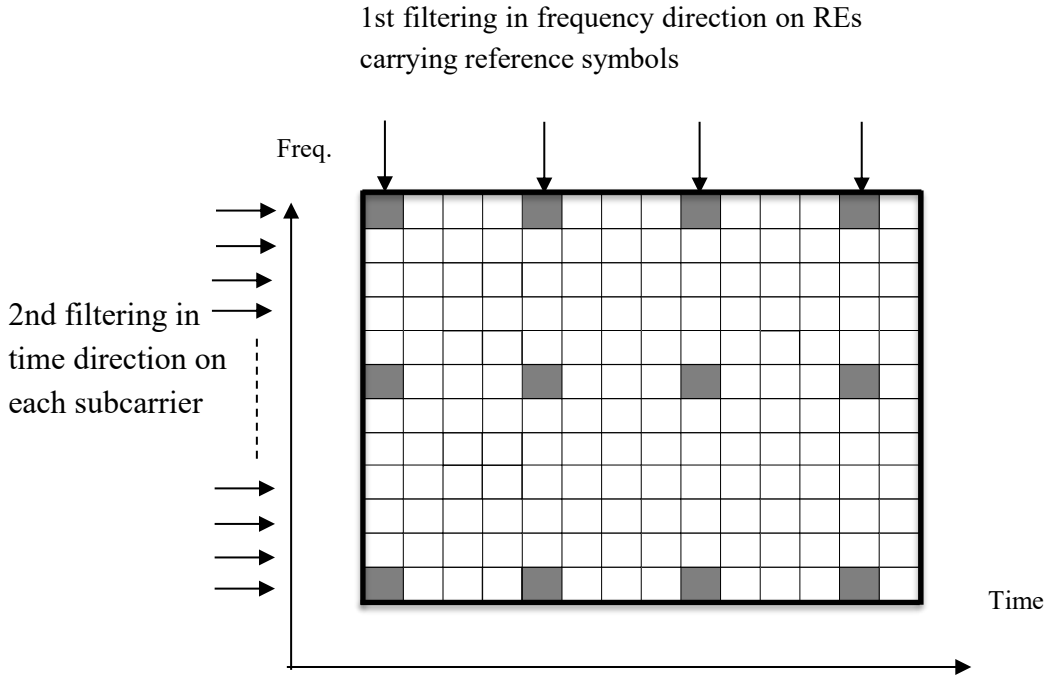

Figure 21. *2× 1-D Wiener filter concept*

For simplicity, consider one transmit and one receive antenna system. Then the received reference symbol is in the form:

$$y_{ref}(f) = h(f)s_{ref}(f) + n(f) \tag{3.6}$$

where $y_{ref}(f)$ is the received reference symbol distorted by channel response $h(f)$, $s_{ref}(f)$ is the transmitted reference symbol, $n(f)$ is AWGN component and f is the sub-carrier index. First the raw channel is estimated on the resource elements carrying reference symbols as follows:

$$h_{raw}(f) = \frac{y_{ref}(f)}{s_{ref}(f)} + \frac{n(f)}{s_{ref}(f)} = h(f) + \hat{n} \tag{3.7}$$

it can be noticed that the raw channel estimate is distorted by the noise component. After the raw channel estimates have been obtained for all reference symbols locations, the first filtering stage in frequency direction can be applied. The output of the first 1-D Wiener filter in frequency direction with coefficients matrix $\mathbf{W}_1$:

$$\widehat{\mathbf{h}_1} = \mathbf{W}_1\mathbf{h}_{raw} \tag{3.8}$$

the coefficients matrix $\mathbf{W_1}$ is of the size $L \times N$ depends on the size of the filter window (L denotes number of subcarriers and N denotes number of the pilots in the estimation window). For example, Figure 21, shows 3 reference symbols in the frequency direction per OFDM symbol in one PRB, so the size of H_{raw} is 3×1 and can be expressed as:

$$\boldsymbol{h}_{raw} = \begin{bmatrix} h_1 \\ h_2 \\ h_3 \end{bmatrix} \tag{3.9}$$

if size of the filter window of the first stage is one PRB, then size of coefficients matrix $\boldsymbol{W}_1$ is 12×3 and can be expressed as:

$$\mathbf{W}_1 = \begin{bmatrix} w_{1,1} & \cdots & w_{1,3} \\ \vdots & \ddots & \vdots \\ w_{12,1} & \cdots & w_{12,3} \end{bmatrix} \tag{3.10}$$

The coefficients matrix of the Wiener filter is calculated to minimize mean square error of the estimation and it can be solved according to [29] to get:

$$\mathbf{W}_1 = \mathbf{R}_{h_{raw}h}\mathbf{R}_h^{-1} \tag{3.11}$$

where $\mathbf{R}_h$ is actual channel auto-correlation matrix and $\mathbf{R}_{h_{raw}h}$ is cross-correlation matrix between raw channel estimates and actual channel response. Both matrices depend on frequency auto-correlation function which is a Fourier transform of the power delay spectrum. Moreover, channel auto-correlation function is calculated using noise variance per subcarrier. So, the output estimate $\widehat{\mathbf{h}_1}$ is of 12×1 size and can be expressed as follows:

$$\widehat{\mathbf{h}_1} = \begin{bmatrix} w_{1,1} & \cdots & w_{1,3} \\ \vdots & \ddots & \vdots \\ w_{12,1} & \cdots & w_{12,3} \end{bmatrix} \times \begin{bmatrix} h_1 \\ h_2 \\ h_3 \end{bmatrix} \tag{3.12}$$

This process is performed in frequency direction on each OFDM symbol that has reference symbols. The coefficients matrix $\mathbf{W}_1$ calculated for the filter window of one PRB can be used to estimate the whole frequency band by sliding the filter window through the whole frequency band. This is possible since the coefficients matrix $\mathbf{W}_1$ is calculated based on correlation properties of propagation channel and interference plus noise statistics. It should be clear that, in this example the frequency domain filter is one PRB window size which can be increased to increase channel estimation accuracy. Increasing window size implies more reference symbols have been taken into account, however it increases computational complexity. The upper bound for window size is channel coherence bandwidth. Similarly, the output of the second 1-D wiener filter in time direction is:

$$\widehat{\mathbf{h}_2} = \mathbf{W}_2\,\widehat{\mathbf{h}_1} \tag{3.13}$$

where $\widehat{\mathbf{h}_1}$ is the channel estimate and $\mathbf{W}_2$ is coefficients matrix of the second filter [18].

It should be clear that in this thesis the channel estimation based on DM-RS and CSI-RS are carried out using the same 2 ×1-D Wiener filter.

3.6 Interference measurement methods

Interference measurement is an important part of UE receiver to cancel out inter-cell interference by calculating interference plus noise covariance matrix. Interference cancellation is essential for the receivers to work optimally specially for the cell edge users where interference power becomes significant. Basically, for demodulation purpose interference plus noise covariance matrix is calculated using DM-RS signal. Then it is used to suppress interference in the MMSE-interference rejection combining (MMSE-IRC*)* receiver discussed later in Section 3.7. While for CSI reports to be prepared, interference can be measured using NZP CSI-RS or CSI-IM signals.

Interference plus noise covariance matrix

Interference plus noise covariance matrix is necessary to build interference-aware receivers. It can be calculated using transmitted reference symbols such as DM-RS, NZP CSI-RS signals or CSI-IM resources where empty resources that collides with the transmission of interfering gNB are used to measure interference. Next CSI-IM and NZP CSI-RS based interference measurements are discussed in detail:

1- CSI-IM based interference measurement

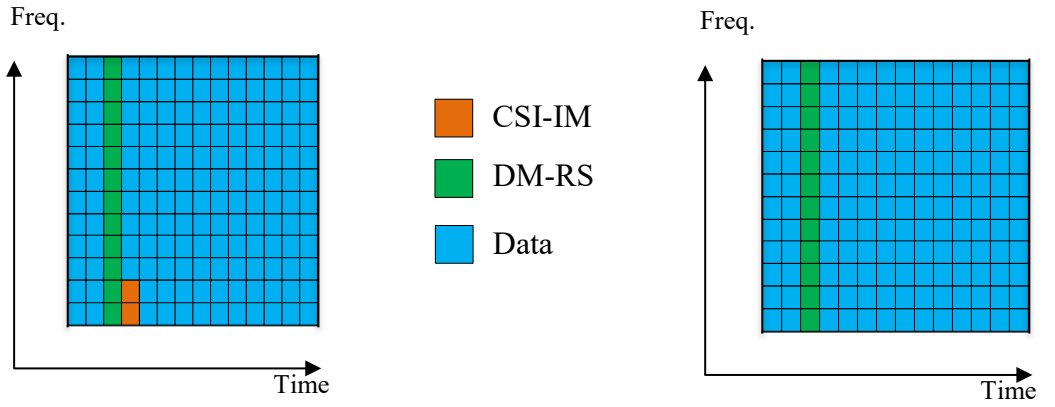

Figure 22. *CSI-IM REs configuration in serving and interfering gNBs*

In Section 3.4, CSI-IM is defined as a set of resource elements in a subframe scheduled by the serving gNB on which UE can measure the interference. Practically, CSI-IM resource elements are covered by ZP CSI-RS to indicate that no data are mapped to these resource elements by serving gNB. Figure 22, shows scheduled subframe of serving gNB, where two CSI-IM resources are allocated in the 4th OFDM symbol colliding with data

resource elements in subframe of interfering gNBs. The received signal on these REs from interfering cells is used by UE to construct interference plus noise covariance matrix as follows. For simplicity only one interferer with one transmit antenna is considered in these calculations. The received signal per CSI-IM resource from interfering gNB can be defined as follows:

$$\mathbf{y}_{interf}(f) = \mathbf{H}_{interf}(f)x_{interf}(f) + \mathbf{n}(\mathrm{f}) \tag{3.14}$$

where $\mathbf{H}_{interf}(f)$ is the channel response of the interfering cell, $x_{interf}(f)$ is interferer transmitted symbol, $\mathbf{n}(\mathrm{f})$ is the noise component and f is the subcarrier index. The received signal from interfering cell does not carry any useful data for the UE. Hence, interference plus noise covariance matrix ($\mathbf{R}$) per CSI-IM RE can be calculated as follows:

$$\mathbf{R} = \mathbf{y}_{interf}(f)\,\mathbf{y}_{interf}(f)^{H} \tag{3.15}$$

where $(.)^{H}$ denotes hermitian (i.e. conjugate transpose) operator. In this thesis, UE is configured with two receive antennas. Therefore, received signal $\mathbf{y}_{interf}(\mathrm{f})$ is in the form:

$$\mathbf{y}_{interf}(f) = \begin{bmatrix} y_1 \\ y_2 \end{bmatrix} \tag{3.16}$$

where y_1 and y_2 are received symbols at antenna ports one and two respectively. Then $\mathbf{R}$ can be expressed as follows:

$$\mathbf{R} = \begin{bmatrix} y_1 y_1^* & y_1 y_2^* \\ y_2 y_1^* & y_2 y_2^* \end{bmatrix} = \begin{bmatrix} \sigma_1 & \sigma_{12} \\ \sigma_{21} & \sigma_2 \end{bmatrix} \tag{3.17}$$

where $\sigma_1$and σ_2 are raw interference plus noise power estimates for the first and second receive antennas respectively. Whereas σ_{12} and σ_{21} represent cross-correlation between antennas one and two. The obtained covariance matrix represents raw interference plus noise covariance matrix per RE of CSI-IM resources. Thus, interpolation in frequency direction is needed to obtain estimates for REs between CSI-IM resources. Moreover, frequency smoothing (interference averaging in frequency domain) is applied to improve the estimation accuracy. The exact description of frequency smoothing is left out of this thesis.

Interference plus noise covariance matrix ($\mathbf{R}$) calculated above, contains interference plus noise power estimates per receive antenna in diagonal elements. Moreover, it contains correlation between receive antennas in off-diagonal elements. So, from now on and for simulations convention, it will be called *CSI-IM full covariance matrix*. If interference is assumed to be fully uncorrelated between receive antennas, then σ_{12} and σ_{21} are set to zero. In this case, $\mathbf{R}$ will be called *CSI-IM diagonal matrix* and can be expressed as follows:

$$\mathbf{R} = \begin{bmatrix} \sigma_1 & 0 \\ 0 & \sigma_2 \end{bmatrix} \tag{3.18}$$

Finally, if interference is assumed to be both spatially and spectrally white and uncorrelated between receive antennas, **R** can be averaged over receive antennas and through all subcarriers. In this case, interference plus noise power can be expressed as single scalar value called *CSI-IM-I_oN_o* [16]. The performance of above mentioned assumptions about interference nature will be evaluated in Section 4.2.

2- NZP CSI-RS based interference measurement

Figure 23. *NZP CSI-RS configuration in serving and interfering gNBs*

Interference measurement can also be performed using the transmitted NZP CSI-RS. Basically, NZP CSI-RS is scheduled so that UE can estimate channel response to prepare CSI reports. However, it can be used to get interference measurement by subtracting the product of estimated channel and transmitted reference symbols that is NZP CSI-RS from the received reference symbols, this approach can be called: residual interference measurement. The term residual stems from the fact that interference measurement is obtained after subtracting the desired signal from the overall received signal. Figure 23, shows scheduled subframe of serving gNB where two NZP CSI-RS resources are allocated on the 4th OFDM symbol colliding with NZP CSI-RS resource elements of subframes of interfering gNBs. The received reference symbol per subcarrier can be represented as:

$$\mathbf{y}_{ref}(f) = \mathbf{H}(\mathrm{f}) s_{ref}(f) + \mathbf{n}(\mathrm{f}) \tag{3.19}$$

where **H**(f) is channel response, $s_{ref}(f)$ transmitted reference symbol and **n**(f) is interference plus noise component and can be calculated as Follows:

$$\mathbf{n}(\mathrm{f}) = \mathbf{y}_{ref}(f) - \mathbf{H}_{est}(f) s_{ref}(f) \tag{3.20}$$

where $\mathbf{H}_{est}(f)$ is estimated channel using NZP CSI-RS. Interference plus noise covariance matrix can be calculated per RE as follows:

$$\mathbf{R}_n = \boldsymbol{n}(f)\,\boldsymbol{n}(f)^H \tag{3.21}$$

The obtained covariance matrix represents raw interference plus noise covariance matrix of the scheduled NZP CSI-RS resources. Thus, interpolation in frequency direction is needed to obtain estimates for REs between NZP CSI-RS resources. Moreover, frequency smoothing (interference averaging in frequency domain) is applied to improve the estimation accuracy. It should be noted that, for both CSI-IM and NZP CSI-RS measurements after covariance matrix is calculated for scheduled REs, then frequency interpolation to get the covariance matrix for the REs between the scheduled one. The last step is to get the measurements for the rest of OFDM symbols in the subframe. This is done by copying the obtained covariance matrix to the rest of REs.

3.7 User equipment receiver

MMSE-IRC

As discussed in Section 3.6, interference measurement is necessary for the receiver to work optimally in scenarios where interference from neighboring cells becomes significant, for example on the cell edge. In MMSE receiver, the weighting matrix **W** is obtained by minimizing the cost function of the mean square error between weighted received and transmitted signal [20]:

$$\mathbf{W}_{MMSE} = \arg\, min_{\mathbf{W}}\, E\{\|\mathbf{W}^H\mathbf{y} - \mathbf{x}\|^2\} \tag{3.22}$$

where $(.)^H$ denotes hermitian (i.e. conjugate transpose) operator. Whereas **y**=**H x** + **r** is the received signal vector, **x** the transmitted signal vector, **r** interference plus noise component and **H** is the channel response matrix. Equation (3.22) can be solved to get Wiener-Hopf equation [30]:

$$\mathbf{W}_{MMSE} = \mathbf{R}_{yy}^{-1}\,\mathbf{R}_{yx} \tag{3.23}$$

where $\mathbf{R}_{yy}$ is received signal auto-correlation matrix, $\mathbf{R}_{yx}$ is cross-correlation matrix of the received and transmitted signals and can be expressed as follows:

$$\mathbf{R}_{yy} = E\{\mathbf{y}\mathbf{y}^H\} = \mathbf{H}\mathbf{H}^H + \mathbf{R} \tag{3.24}$$

$$\mathbf{R}_{yx} = E\{\mathbf{y}\mathbf{x}^H\} = \mathbf{H} \tag{3.25}$$

where **R** is interference plus noise covariance matrix explained in Section 3.6. So, equation (3.23) can be written as:

$$\mathbf{W}_{MMSE} = (\mathbf{H}\mathbf{H}^H + \mathbf{R})^{-1}\mathbf{H} \tag{3.26}$$

Then the detected symbol is in the form:

$$x_{MMSE} = \mathbf{W}_{MMSE}{}^{H}\mathbf{y} \tag{3.27}$$

It should be noted that the MMSE-IRC receiver ability to suppress inter-cell interference depends on the accuracy of interference measurement. The accuracy of interference measurements depends on interference estimation algorithm, the reference symbol used, number of reference symbols used and the availability of the channel knowledge of interfering cells. The more accurate the interference can be estimated, the more interference can be suppressed. Therefore, the better detection capability of the receiver.

3.8 Channel quality indicator

As mentioned earlier, LA performance is greatly affected by the quality of CQI reports. CQI provides recommendations about the next transmission modulation scheme and code rate so that a certain target BLER is achieved. The ideal CQI report is to send absolute SINR on a PRB basis. This approach provides very accurate information to LA, but it is not practical as it implies a very high uplink overhead. Different schemes are proposed to reduce the overhead for CQI reports, see e.g. [28]. In Release 15, 3GPP has standardized two CQI tables with 15 indices each. This allows to report CQI using 4 bits in the uplink transmission. The first table supports up to 64 QAM and the second table supports up to 256 QAM [26]. Table 5, shows the first table with CQI index and SINR switching threshold with 10% target BLER for the corresponding MCS.

Table 5. *CQI indices up to 64QAM*

CQI Index	Modulation order	Code Rate × 1024	SINR threshold (dB)
0	No transmission		
1	QPSK	78	-9.478
2	QPSK	120	-6.658
3	QPSK	193	-4.098
4	QPSK	308	-1.798
5	QPSK	449	0.399
6	QPSK	602	2.424
7	16QAM	378	4.489
8	16QAM	490	6.367
9	16QAM	616	8.456
10	64QAM	466	10.266
11	64QAM	567	12.218
12	64QAM	666	14.122
13	64QAM	772	15.849
14	64QAM	873	17.786
15	64QAM	948	19.809

CQI calculations

In general, down link channel quality is measured by post detection SINR at the UE. Next CQI calculation scheme used in this thesis is explained. It should be noted that there are different schemes proposed for CQI calculations as it is not part of 3GPP standard. In this thesis CQI is calculated as follows: Firstly, channel condition is measured using the scheduled NZP CSI-RS signal or by ideal channel estimation. Then interference plus noise is estimated using the scheduled CSI-IM or NZP CSI-RS signals. Channel and interference measurements are explained in sections 3.5 and 3.6 respectively. The post detection SINR per RE of the received signal is calculated using MMSE-IRC receiver. MMSE-IRC receiver uses calculated channel and interference measurements for the detection purpose. As mentioned above, it is not practical to report the post detection SINR per RE as it implies a lot of signaling overhead. So, to perform the feedback an average value represents link quality is calculated. In this thesis, mean mutual information per bit (MMIB) is used as link quality metric. Post detection SINRs are mapped to MIBs values using pre-calculated and stored lookup tables. Then MMIB is obtained by getting the average MIB value of the total number of REs. The obtained MMIB is used to get the MCS that delivers the highest throughput (TP) by looping through 28 MCS indices table.

For example, starting from the first index in Table 4, number of transmitted bits is calculated then code block size (CBS) is calculated as a function of modulation order and code rate (CR). Then using BLER prediction (estimation) algorithm defined in [22], BLER is estimated for this transmission parameters CBS, CR and MMIB as inputs. Estimated BLER is used to calculate TP. This TP is stored and then compared to the obtained TP of the next MCS index until the highest possible TP and corresponding MCS is found. Then the obtained MCS is mapped to the closest CQI index. Finally, BLER is estimated for the selected CQI to ensure that the target BLER is achieved. If the estimated BLER is larger than the target BLER, the selected CQI index is reduced by one.

3.9 Channel and interference measurement configurations

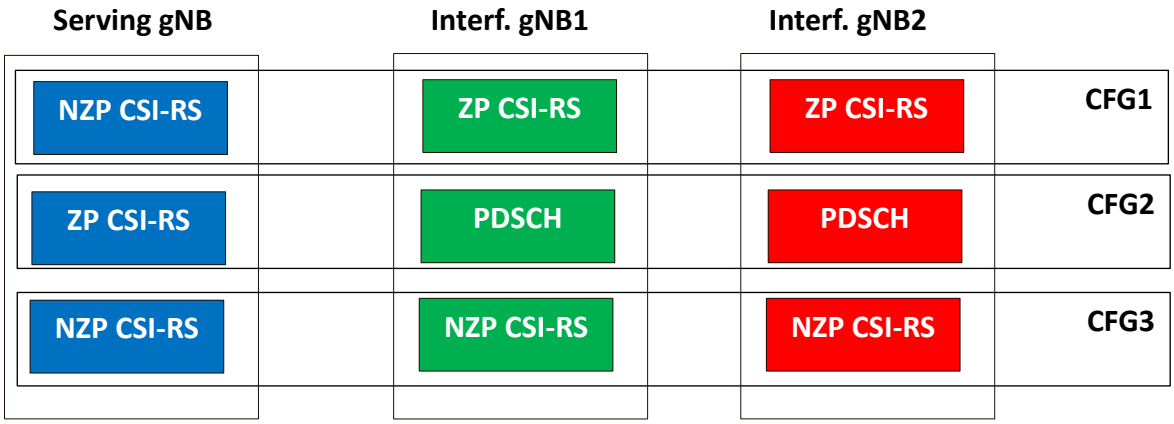

Figure 24. *Channel and interference measurement configurations.*

In this section, three different configurations are provided that will be used in the simulations carried out to conduct this study. CSI-IM based interference measurement method will be performed using the first and second configurations denoted as CFG1 and CFG2 in Figure 24. The first configuration is intended for channel measurement used for CQI calculations. In this configuration NZP CSI-RS is scheduled in the subframe of the serving gNB and it is colliding with ZP CSI-RS of interfering gNBs. This configuration allows the UE to get clean channel estimation. The term clean refers to the fact that the NZP CSI-RS resources of serving gNB are not interfered by another gNBs transmission as they are colliding with ZP CSI-RS resources. Recall that ZP CSI-RS signals refers to the set of REs where no data channel is scheduled. The second configuration allows UE to measure interference from another gNBs. The subframe of the serving cell is scheduled by CSI-IM resources and ZP CSI-RS is scheduled on the same resources, so no data is scheduled on these resources. CSI-IM resources are colliding with data channel (PDSCH) resources of interfering gNBs and interference can be measured. NZP CSI-RS based interference measurement will be performed using the third configuration denoted as CFG3 in Figure 24. In the third configuration, NZP CSI-RS scheduled in the subframe of the serving gNB is colliding with NZP CSI-RS of interfering gNBs [19]. This configuration allows UE to get both channel and interference measurements required for CQI calculations is explained in Section 3.6.

4. RESULTS AND ANALYSIS

In this chapter, Link level simulation results to evaluate the performance of proposed interference measurement methods are introduced. General settings and simulation assumptions are introduced in Section 4.1. In Sections 4.2 and 4.3 link level simulations and results in terms of downlink data channel (PDSCH) throughput against SINR is introduced. These results evaluate the performance of two RS-based interference measurement methods using different channel models and UE speeds. Moreover, different REs density per PRB, CSI periodicities and frequency granularities are studied. In Section 4.4, comparison between previously studied RS-based interference measurement are studied. Finally, in Section 4.5, overall system overhead is studied.

4.1 Simulation assumptions

In this section, link level simulation assumptions are introduced. The performance of different interference measurement methods is studied. The performance metric is the downlink data channel throughput (TP). Basically, PDSCH TP which is the number of successful received data bits per second as a function of SINR. The number of transmitted bits in one subframe depends on the modulation order, code rate of transmitted bits and the number of resource blocks in the downlink transmission assigned to UE. Moreover, in NR different subcarrier spacings implies different number of slots within subframe. So, for higher subcarrier spacings there are more slots in the subframe which means higher number of transmitted bits. The general simulation assumptions and parameters are configured as follows:

- One serving cell carrying out downlink data transmission to a single UE.
- Two interfering cells with one dominant interferer and one weaker interferer following INR3 profile [23].
- All gNBs are transmitting PDSCH on the whole bandwidth and no empty resources.
- Only PDSCH is scheduled i.e. no control channel or broadcast channel is scheduled.
- Ideal channel estimation is performed for demodulation purpose and CQI calculations.
- Minimum mean square error with interference cancellation (MMSE-IRC) is used for equalization.
- Serving cell has adaptive modulation and coding (AMC) scheme enabled, following reported CQI from UE. Interfering cells are having MCS of index 5 (QPSk).
- Propagation channel models are based on 3GPP channel models tdl-a-30ns and tdl-c-300ns.
- UE speeds are 3 or 30 kmph.

- All gNBs have two transmit antennas and the UE has two receive antennas.
- The number of assigned PRB is 100 corresponds to 20 MHz system bandwidth with subcarrier spacing being used is 15 kHz.

Table 6. provides simulation parameters of the simulated curves.

Simulation reference curve

Reference curve is configured as the most optimal configuration, yet not a practical one. This configuration is optimal in a sense that, same interference plus noise covariance matrix is used for interference cancellation for demodulation process and in CQI calculations. This covariance matrix is calculated based on DM-RS signals. The reason behind this is to match the reported CQI and receiver demodulation capabilities, since both processes are using the same covariance matrix. Moreover, in reference curve CSI is reported every subframe and available immediately in gNB without delay. On the other hand, reference curve is not practical, since DM-RS is only transmitted whenever there is data scheduled for transmission. Furthermore, it is transmitted in the same data bandwidth, so it can't support wideband CSI reports since the data transmission has variable bandwidth depending on the amount of data to be transmitted. Also, DMRS is transmitted from the same antenna ports as data channel (PDSCH), but CSI-RS can be transmitted from all antenna ports, regardless of PDSCH antenna ports.

Practical curves use CSI-IM or NZP CSI-RS based interference measurement in CQI calculation. This will result in reported CQI higher or lower than demodulation capability at the receiver. Moreover, there is a delay of one subframe between when CQI is calculated and reported back to gNB. In practical curves CSI reports are transmitted at predefined periodicities of 5, 10, 20 or 40 ms.

Table 6. *Simulations assumptions*

Parameter	Reference curve	Practical curve
Carrier frequency	4 GHz	4 GHz
Bandwidth	20 MHz (100 PRBs)	20 MHz (100 PRBs)
Transmission method	single-layer-two-antenna-port	single-layer-two-antenna-port
Antenna configuration	gNB: 2, UE: 2	gNB: 2, UE: 2
Subcarrier spacing	15 kHz	15 kHz
Channel model	tdl-a-30ns/tdl-c-300ns	tdl-a-30ns/tdl-c-300ns
UE speed	3, 30 kmph	3, 30 kmph
Channel coding	LDPC	LDPC
Channel estimation	Ideal channel estimation	Ideal channel estimation
Receiver algorithm	MMSE-IRC	MMSE-IRC
Number of interfering gNBs	2	2
DIP profile for INR3	[-0.524416 -11.09441] dB	
CSI reports		
Delay in SF	0	1
Periodicity in SF	1	5/10/20/40 ms
Channel estimation	Ideal channel estimation	Ideal channel estimation
Interference measurement	Based on DM-RS	Based on CSI-IM and NZP CSI-RS

It should be noted that in order to evaluate interference measurement quality and accuracy in the next Sections 4.2 and 4.3, ideal channel measurement is used to prepare CQI reports. In other words, the accuracy of calculated CQI will depend only on the quality of interference measurement.

4.2 CSI-IM based interference measurement

In this section, link level simulations are carried out to evaluate the performance of CSI-IM based interference measurement. Basically, the same subframe configuration defined in Figure 22, is used in this simulation. Where two CSI-IM REs per PRB are scheduled in the subframe of the serving cell. These REs are colliding with data channel of interfering cells. In this section, the concept of interference averaging is introduced as a technique used to increase the accuracy of the measurements. Different factors that affects the performance are investigated such as, assumptions about interference nature, reference symbols periodicity, number of REs per PRB and frequency domain granularity.

Interference averaging

In Section 3.3, inaccuracies of CQI calculations are discussed and OLLA is proposed to correct for these inaccuracies at the base station. Interference averaging is another technique that aims to mitigate measurement errors at the UE before CQI is calculated. There are different ways to perform interference averaging, but in this thesis a scheme provided in [31] is adopted. In this scheme, the current measurement ($I_{current}$) is related to the previous measurement (I_{prev}) by forgetting factor α as follows:

$$I = \alpha I_{prev} + (1 - \alpha) I_{current} \tag{4.1}$$

where forgetting factor α is configurable parameter to be determined for each system. It should be noted that no interference averaging is performed if forgetting factor equals to zero. Figure 25, shows that proper choice of forgetting factor α will bring performance gain to LA process and improves the overall TP for the cell edge user.

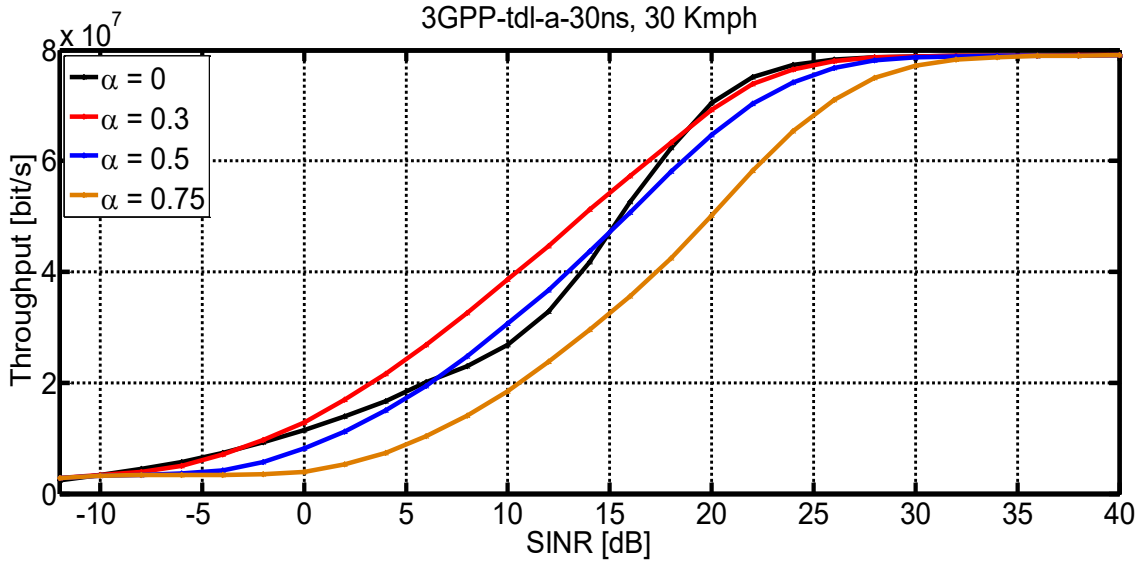

Figure 25. *Forgetting Factor (α) choice*

In Figure 25, the performance of CSI-IM based interference measurement with different α values are shown. The goal is to determine the value that results in the best overall performance under the given channel model, interference profiles and UE speed (30 kmph). It shows that α equal to 0.3 that is 30% of the previous measurement (red curve) results in the highest performance among the other α values. Hence, α equal to 0.3 will be used from now on as interference averaging parameter for CSI-IM based interference measurement.

Assumptions about interference nature

In Section 3.6, it has been explained that interference plus noise covariance matrix **R** can be used in CQI calculations with three different assumptions about interference nature. If spectral, spatial characteristics of interference and correlation between receive antennas to be considered in the calculations, then *full covariance matrix* is used. Moreover, if correlation between receive antennas is not considered then off-diagonal elements are set to zero and *diagonal matrix* is used. Finally, if interference is assumed to be both spectrally and spatially white and fully uncorrelated between receive antennas then a single scalar value I_oN_o is used.

In Figure 26a, INR3 profile is used, that maps to DIP profile of [-0.524416 -11.09441] dB explained in Section 3.1. It shows that *full covariance matrix* has the best performance among the other interference assumptions. This is because full covariance matrix reflects complete interference characteristics. Diagonal matrix shows slightly better performance than "IoNo_{est}" over the whole SINR regime as it contains antenna port specific interference plus noise power. While I_oN_o curve represents the average interference plus noise power across receive antennas and subcarriers. This implies losing a lot of information about interference nature, that leads to the lowest performance compared to other interference assumptions. So, from now on *full covariance matrix* will be used in the simulations. It should be noted that under strong interference scenarios full covariance matrix is the best choice to be used in CQI calculations. While in weak interference scenarios the three different assumptions will result in the same performance. In Figure 26b, a weak interference scenario is assumed with DIP profile of [-7 -10] dB. It shows that under the given weak interference profile three different interference assumption will result in the same performance. This is because interference powers are very weak that it is comparable to noise levels. So, single scalar value can be used to represent interference plus noise power without causing performance drop.

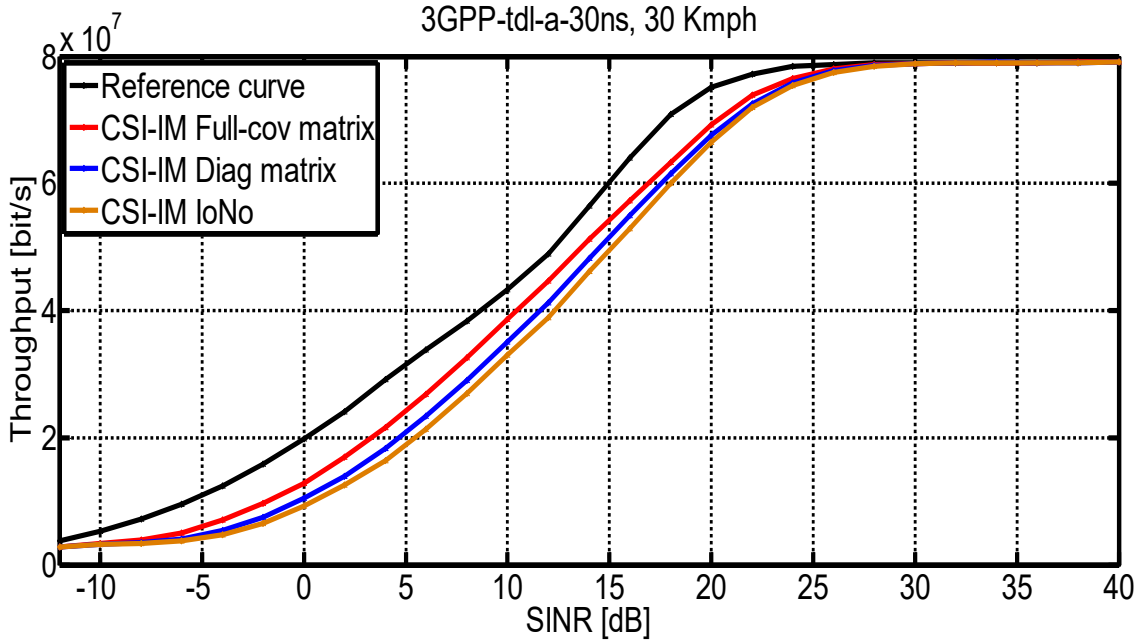

(a) DIP profile = [-0.524416 -11.09441] dB

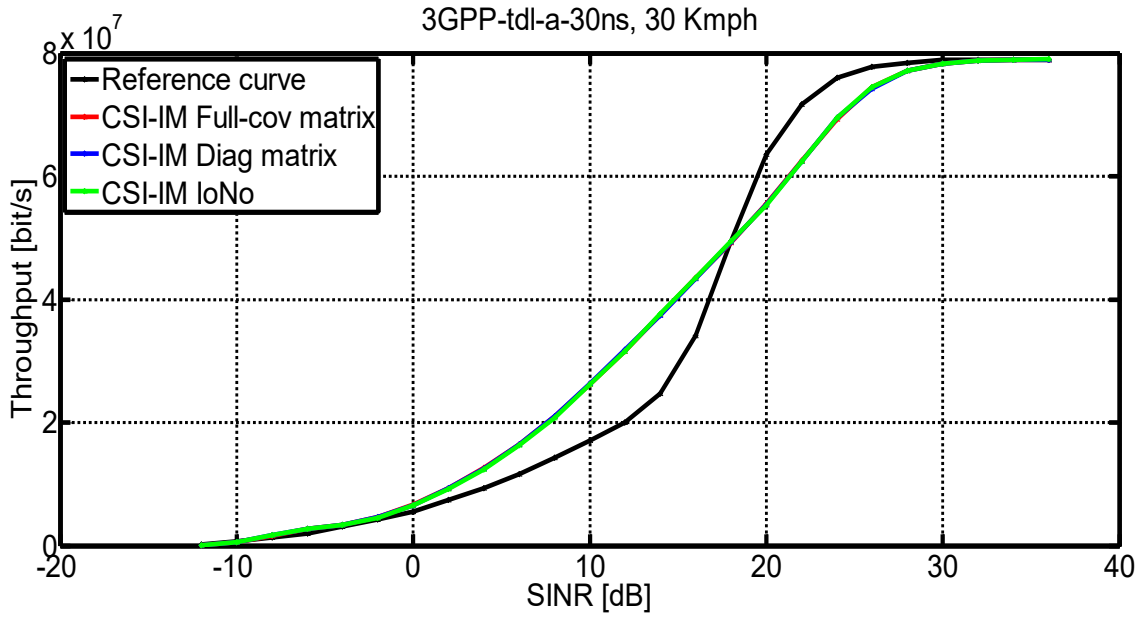

(b) DIP profile = [-7 -10] dB

Figure 26. *Performance of Different assumptions about interference nature, two DIP profiles are tested defined in Section 3.1*

CSI-IM Signal periodicity

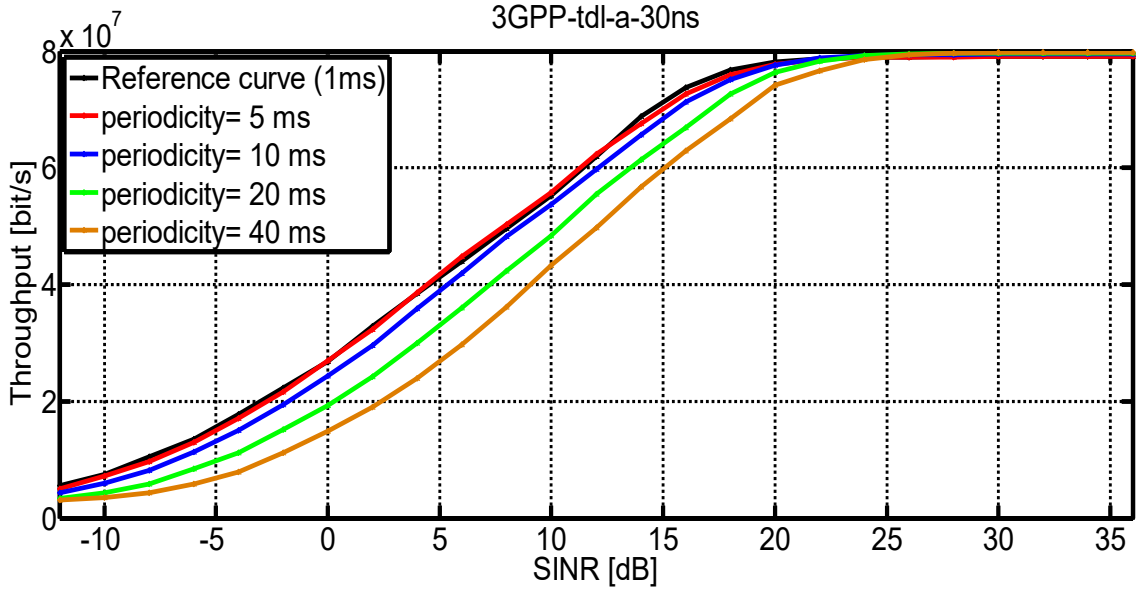

(a) UE speed = 3 kmph

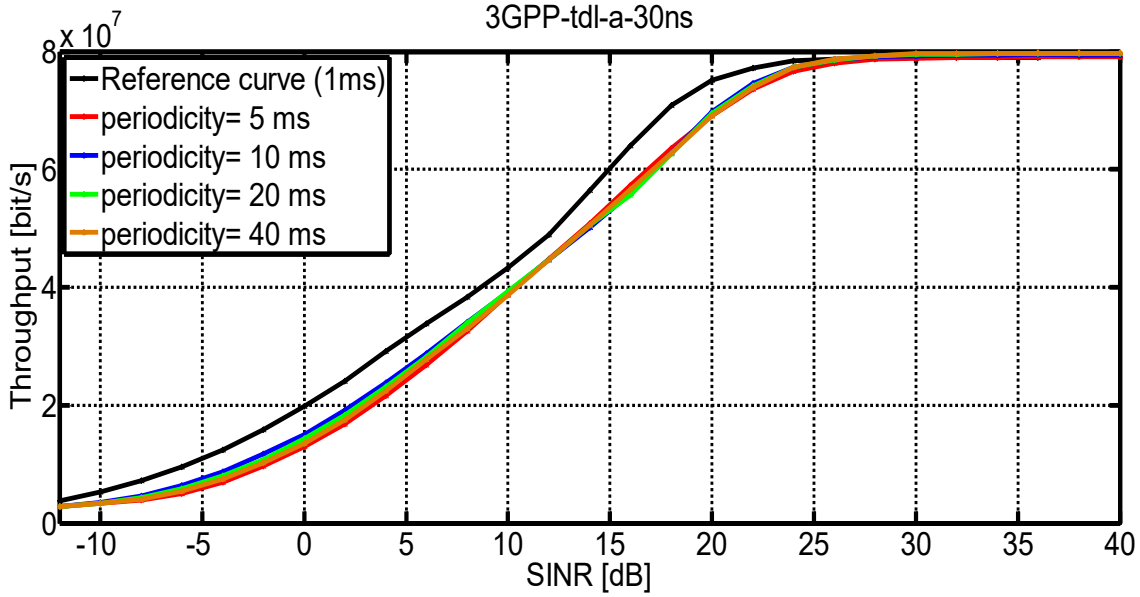

(b) UE speed = 30 kmph

Figure 27. *Performance of different CSI-IM signal periodicities with two UE speeds= 3,30 kmph.*

As mentioned earlier in Section 3.4, CSI-IM resources can be scheduled with different periodicities. It can be scheduled twice every frame up to every 64 frames, i.e. 5 ms and 640 ms respectively. Figure 27, compares between four different periodicities 5, 10, 20 and 40 ms in two different user mobility cases where UE speeds are 3 and 30 kmph. Channel variations in time domain due to user mobility strongly affects LA performance. Coherence time (T_C) defines the time duration over which the channel time correlation is

more than 50% and it can be calculated using the following approximation: $T_C \approx \frac{9}{16\pi f_d}$, f_d is the maximum doppler spread $f_d = f_c \frac{v}{c}$, where f_c is carrier frequency which is 4 GHz in this evaluation, v is UE speed and c is speed of light.

As can be seen from Figure 27 a, where UE speed is 3 kmph coherence time is equal to 16.1 ms, therefore first two periodicities 5 and 10 ms will be reporting in a time window less than coherence time so the reported CQI is following channel variations. Moreover, interference powers are also varying with the channel variations of interfering cells. So, reporting periodicities less than T_C will get more accurate interference measurements. Figure 27 a, shows that 5 ms periodicity has slightly higher throughput in the operating SINR range than 10 ms. At 70% of maximum throughput 5 ms periodicity curve has 0.71 dB gain over 10 ms periodicity curve. In case of 20 and 40 ms periodicities reported CQI will be outdated as the channel coherence time is less than CSI periodicity, resulting in an observable performance degradation compared to 5 ms case. At 70 % of maximum TP 5 ms curve 3.75 dB gain over 40 ms curve. This is because the channel response of interfering cells has been changed resulting different interference levels at the UE.

In Figure 27 b, UE speed is 30 kmph resulting in 1.6 ms coherence time so all curves are using out dated CQI resulting in overall same performance. In this case using higher periodicity to lower down reference signals overhead is recommended.

CSI-IM density

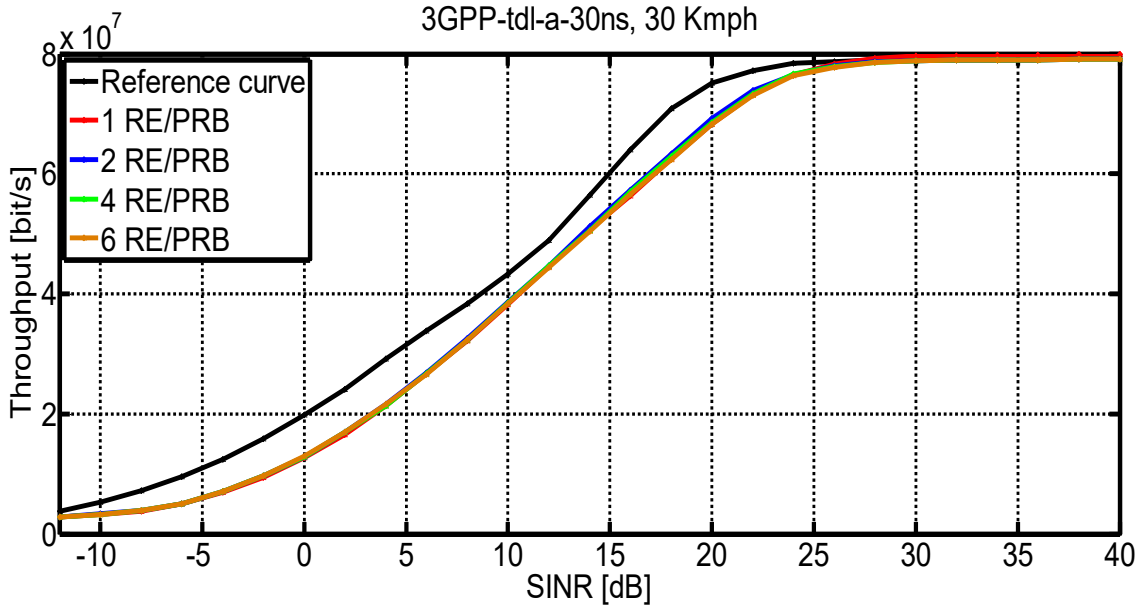

Figure 28. *Number of CSI-IM REs/PRB*

CSI-IM density refers to the number of CSI-IM REs allocation per physical resource block (RE/PRB). Figure 28, compares between different CSI-IM densities. The overall

performance shows that scheduling more resource elements in PRB to measure the interference of interfering cells do not improve the performance. In contrast, it contributes to the system overhead. The fact that introducing more REs to measure interference has no gain in system performance is because the frequency separation between CSI-IM REs is less than channel coherence bandwidth. So, frequency characteristics of the interference are captured.

CSI-IM frequency domain granularity

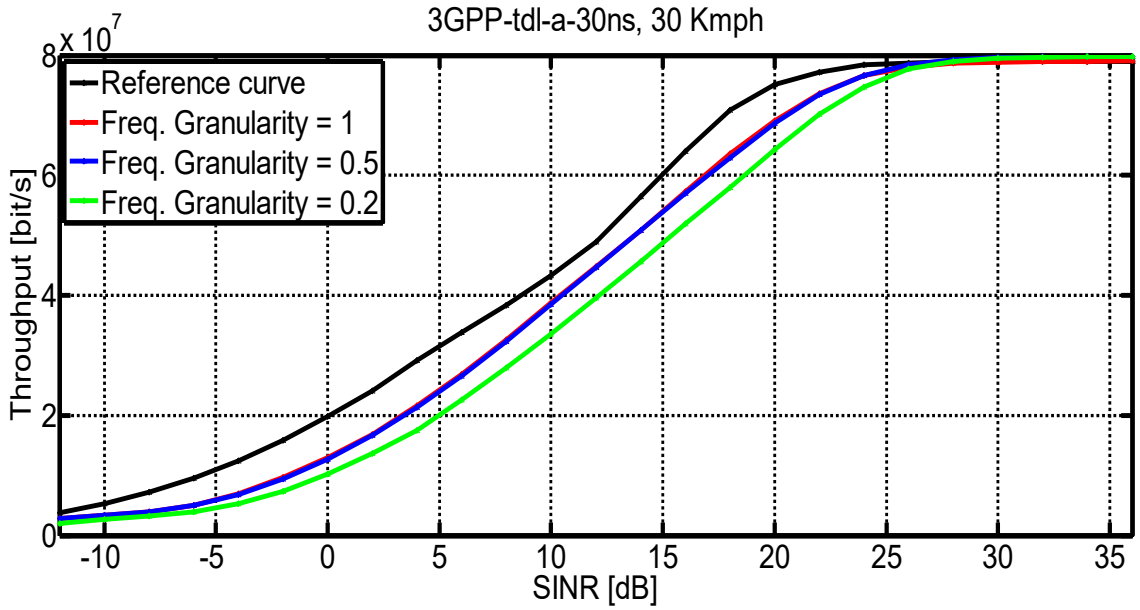

Figure 29. *Interference measurement performance with different CSI-IM frequency domain granularity*

Frequency domain granularity refers to the rate at which CSI-IM resources are allocated in frequency domain per PRB basis, for example if frequency granularity (FG) is one, this means CSI-IM resources are allocated in every PRB within the system bandwidth and if FG is 0.5 this means CSI-IM is allocated every two PRB in frequency domain, and so on. According to 3GPP standard CSI-IM REs are scheduled in every PRB in frequency domain [10]. Figure 29, compares between three different frequency granularities 1, 0.5 and 0.2. It shows that scheduling CSI-IM resources every two PRB (FG = 0.5) will maintain the same performance of FG = 1. In this case, less system overhead compared to scheduling CSI-IM every PRB is the gain. However, reducing it to every five PRB (FG = 0.2) will result in observable performance drop. This configuration will result in less accurate interference measurement, since channel variations of interfering cells are not captured by CSI-IM resources.

4.3 NZP CSI-RS based interference measurement

In Section 3.6, NZP CSI-RS based interference measurement is explained in details. Where NZP CSI-RS resources are first used to get channel measurement to prepare CSI reports. Then it can be used to perform interference measurement at UE. This can be done by subtracting the estimated channel multiplied by transmitted reference symbols (i.e. NZP CSI-RS) from the received reference symbols. However, it should be clear that in this section ideal channel measurement is used to calculate CQI, so only interference measurement can be evaluated. Simulation assumptions used to carry out NZP CSI-RS simulations follows the same general assumptions introduced in Section 4.1.

Interference assumptions

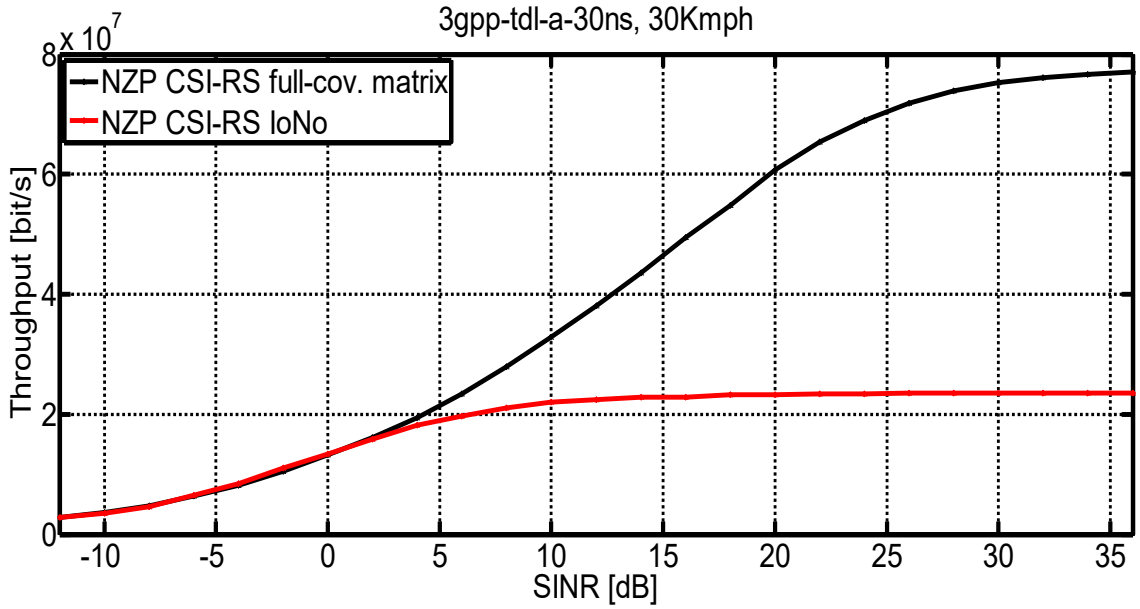

Figure 30. *Performance comparison between full interference plus noise covariance matrix and single scalar value of interference power IoNo*

Figure 30, shows that there is significant performance drop when using single scalar value (I_oN_o) to represent interference plus noise power compared to full covariance matrix representation. This is because full covariance matrix contains the complete characteristics of the interference. Both spectral and sptail charactersistics are included, in addtion to correlation between receive antennas. While I_oN_o is calculated assuming that interference is both spectrally and spatially white and the receive antennas are full uncorrelated. So, a lot of interference information is lost by averaging to get the single scalar value. So, from now on full covariance matrix is used in the simulations.

User mobility

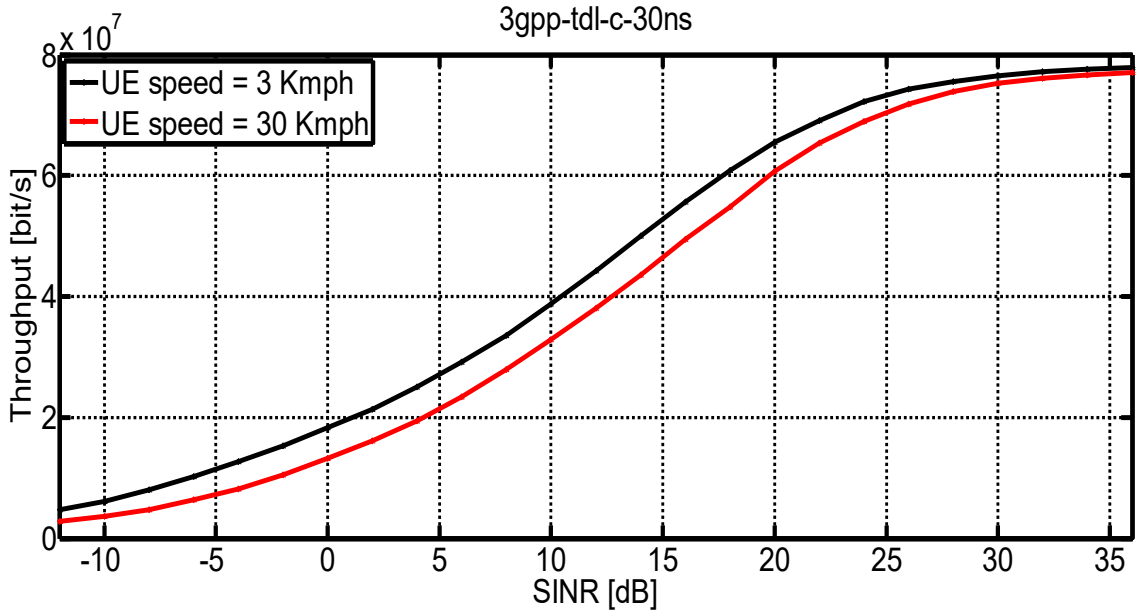

Figure 31. *Effect of UE speed on interference measurement*

User mobility defines the speed of UE, which is directly related to time nature characteristics of radio channel. Users with high mobility will experience fast changing channel conditions. In this simulation setup, two NZP CSI-RS REs are allocated in the 4th OFDM symbol. So, in case of time varying channel conditions one OFDM symbol allocation per subframe maybe not enough to track channel variations of interfering cells. This will affect the accuracy of interference measurement since the interfering signal powers are changing with the channel variations of interfering cells. In other words, if the channel conditions of interfering cells are good, so the received interference power will be high and vice versa. Figure 31, shows the effect of user mobility on the delivered TP to UE, where two user speeds are evaluated: 3 and 30 kmph. It can be seen that user with 30 kmph has lower TP compared to 3 kmph user over SINR regime. This can be explained since the current configuration is not able to follow the time variations on interference powers due to fast varying channel conditions of interfering cells. In this case, scheduling NZP CSI-RS REs in more than one OFDM symbol could improve interference measurement. Scheduling more REs in time domain with separation less than T_C could improve interference measurement by following the time variations of received interferer signal. However, as a downside increasing the number of NZP CSI-RS REs would increase the system overhead.

Periodicity

Similar to CSI-IM configurations, NZP CSI-RS can be scheduled with different periodicities ranging from 5 up to 640 ms. In Figure 32, UE speed equals 3 kmph that coressponds to T_C of 16.1 ms as calculated earlier in this chapter. It compares between 4 different periodicities 5, 10, 20 and 40 ms. It is clear that, curves with 5 and 10 ms periodicities are operating within T_C window resulting in nearly the same performance so, a 10 ms periodicity can be used under the given assumptions to reduce system overhead. On the other hand, 20 and 40 ms curves starts to use an outdated measurement in the time window higher than T_C untill the new measurement takes place. This will result in outdated CQI in gNB which in turn affects system performance.

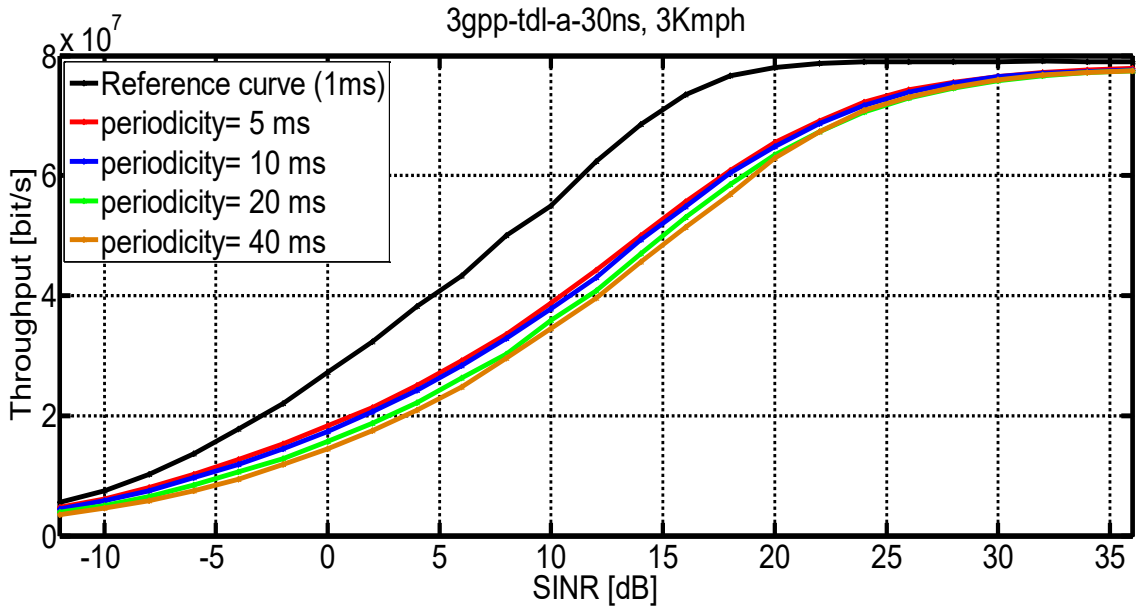

Figure 32. *Performance of different NZP CSI-RS signal periodicities with UE speed = 3 kmph*

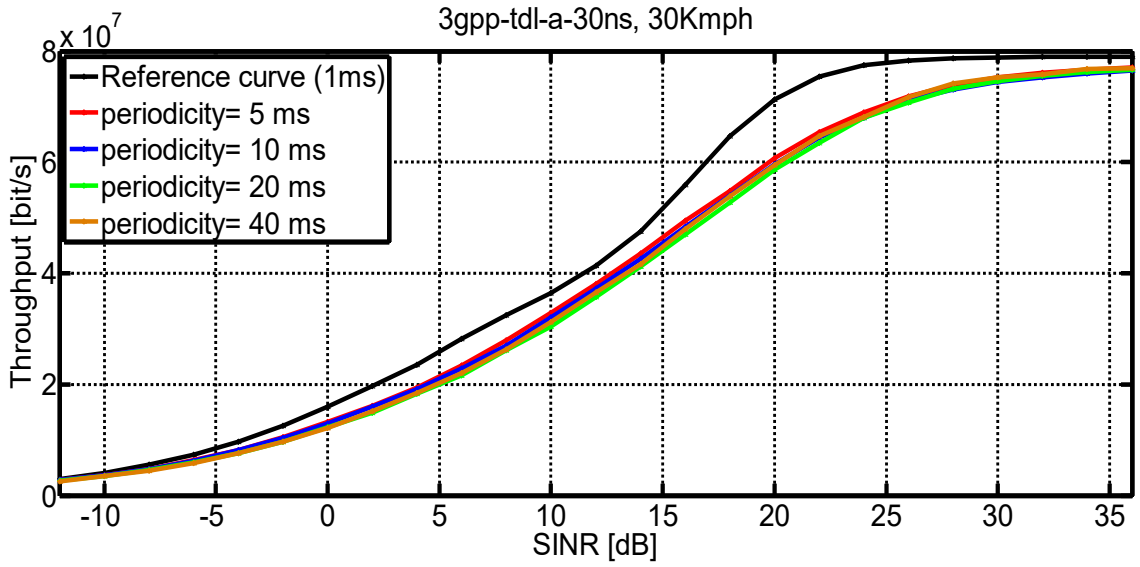

Figure 33. *Performance of different NZP CSI-RS signal periodicities with UE speed = 30 kmph*

In Figure 33, the UE speed is 30 kmph that coressponds to T_C equals 1.6 ms. So, all intereference measurements are not following the time varation of interfering signal resulting in overall same perfromance.

NZP CSI-RS frequency domain granularity

NZP CSI-RS is scheduled every PRB in frequency domain following 3GPP standard for NR. To study the posibility of reducing system overhead by using lower FG, Figure 34 shows a significant performance drop when scheduling NZP CSI-RS resources every two and five PRB (blue and green curves respectively). This indicates that interference power variations due to changing channel conditions in frequency domain of interfering cells are not well captured. This will reduce the accuracy of interference measurement.

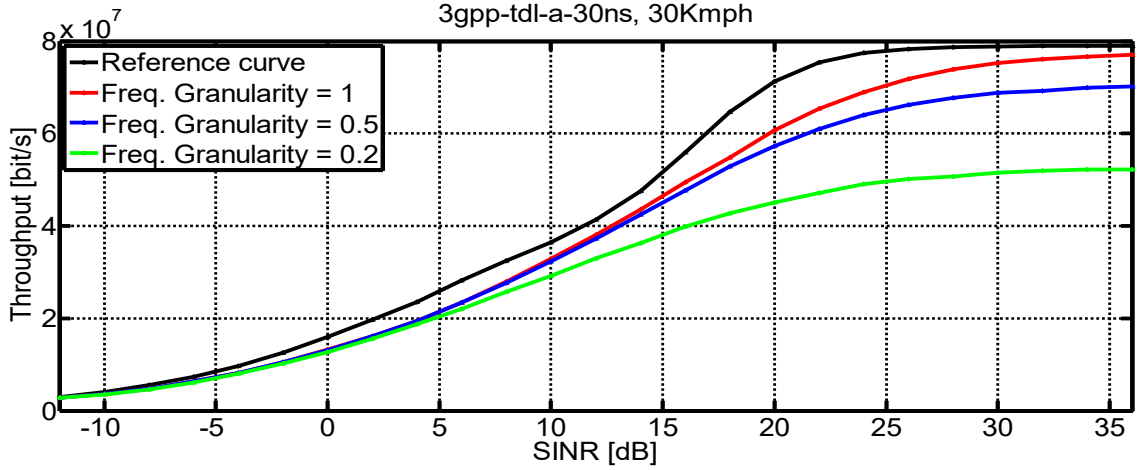

Figure 34. *NZP CSI-RS frequency domain granularity*

NZP CSI-RS density

Similar to CSI-IM, NZP CSI-RS density refers to the number of REs scheduled per PRB (RE/PRB). Figure 35, compares between 2,4 and 6 RE/PRB. It shows that in a frequency non-selective channel model 3GPP tdl-a-30ns, three different densities have the same performance. This is due to the frequency separation between NZP CSI-RS resources is less than channel coherence bandwidth of interfering cells. So, interference powers can be measured accurately with 2 REs/PRB. On the other hand, in a frequency selective channel model 3GPP tdl-c-300ns, increasing number of scheduled RE/PRB improves the overal performance, but it is clear that up to 6 REs/PRB are not enough to get similar performance compared to non-selective channel case.

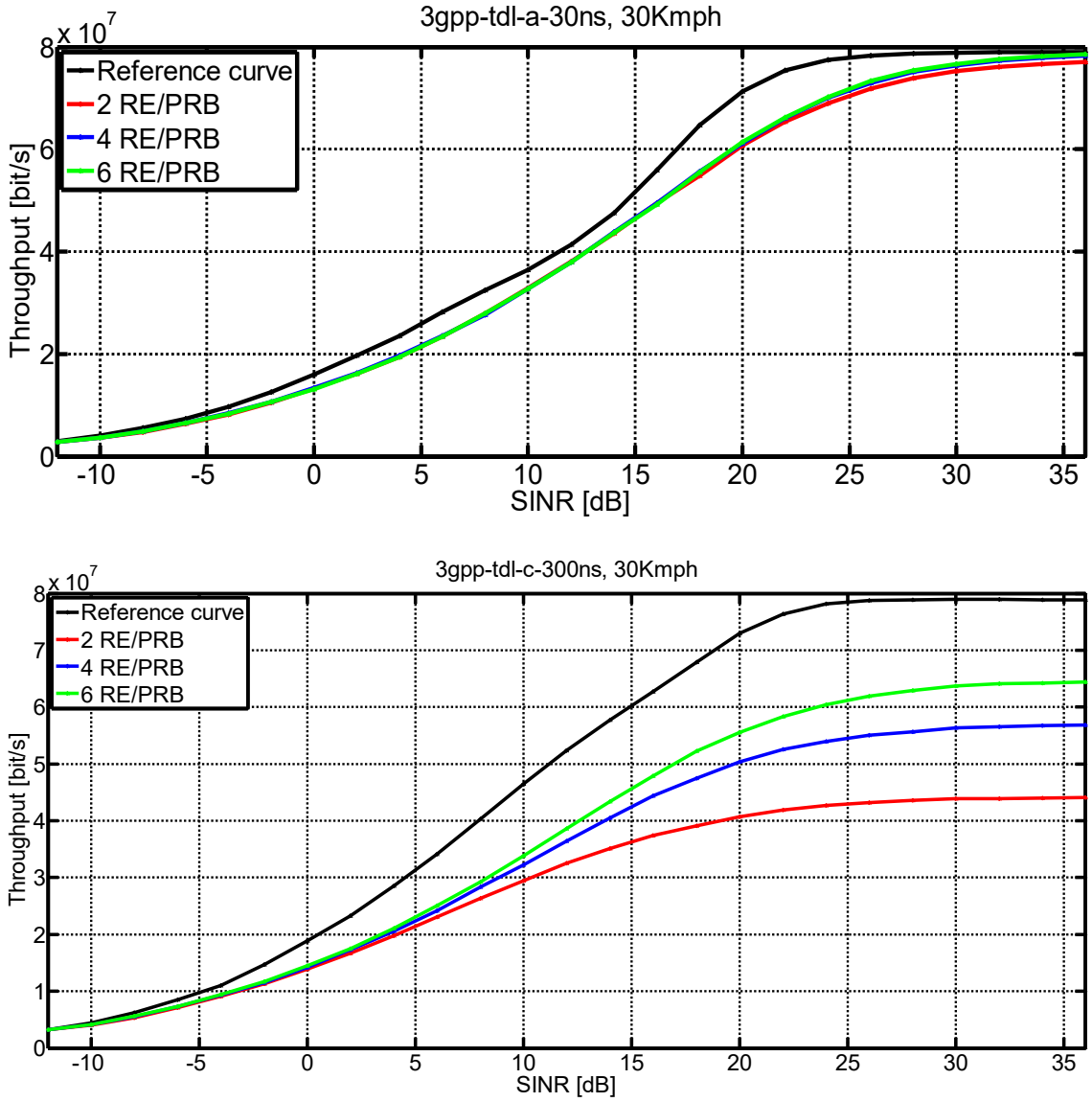

Figure 35. *Number of NZP CSI-RS REs/PRB*

Channel selectivity

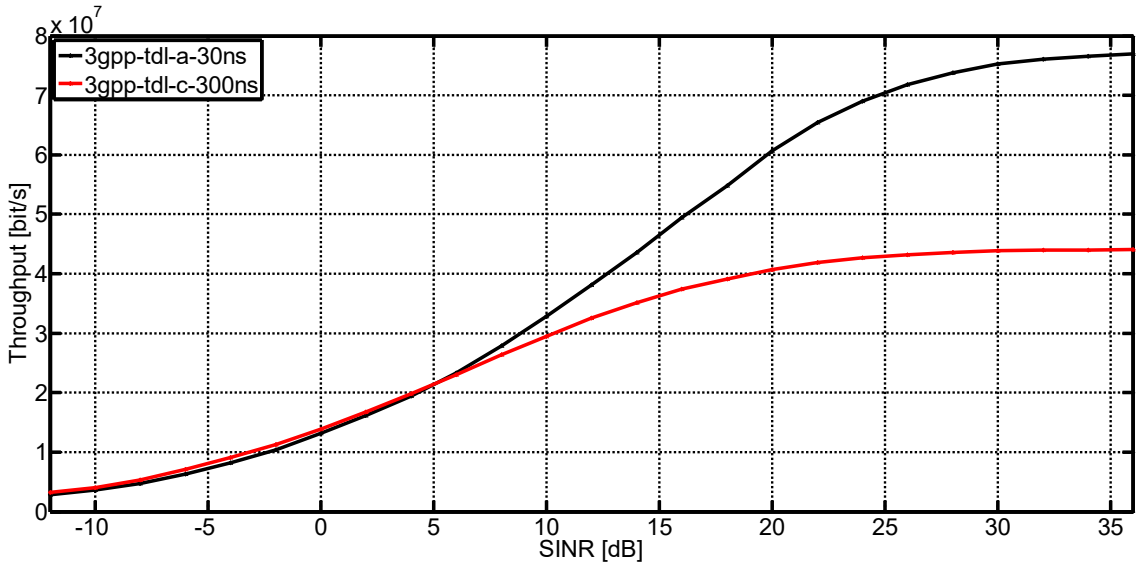

Figure 36. *Channel selectivity effect on Interference measurement*

Figures 34 and 35, have shown that NZP CSI-RS based interference measurement is very sensitive to channel varations of interfering cells. Figure 36 compares the performance under two different channel models. It shows that with frequency selective channel model (red curve) that is 3GPP tdl-c-300ns, the current NZP CSI-RS configuration with 2 REs/PRB are not enough to obtain accurate interference measurement. This results in a very poor throughput performance compared to the case of non- selective channel model. Hence, to improve the performance more REs/PRB need to be scheduled to follow the interference power variations due to channel selectivity of interfering cells .

4.4 Interference measurement methods comparison

In previous sections the performance of CSI-IM and NZP CSI-RS interference measurement methods were studied. Next performance evaluation comparison between these two methods are introduced with the same simulation assumptions defined in Section 4.1.

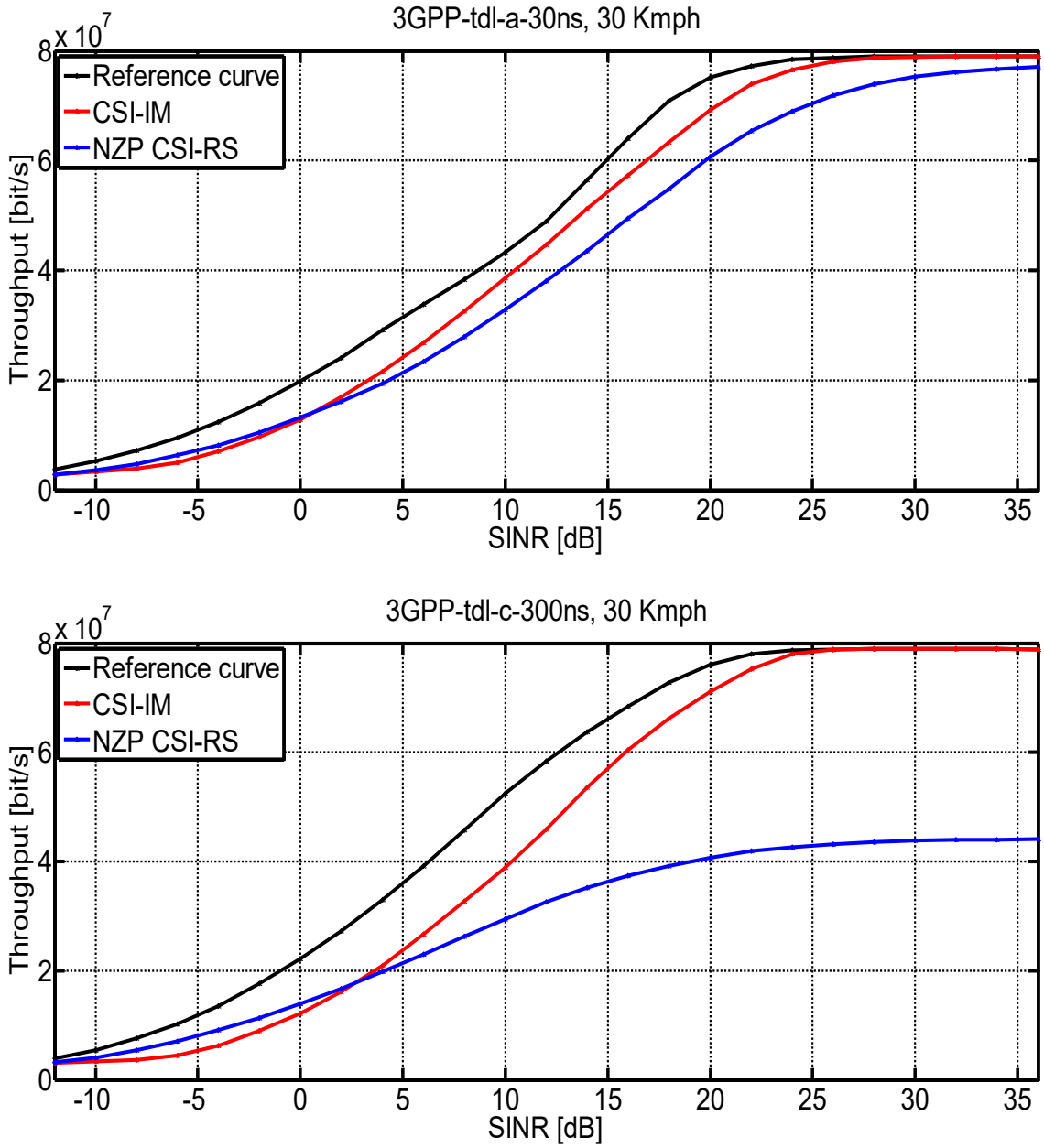

Figure 37. *RS interference measurement comparison with channel model: 3gpp tdl-a-30ns, tdl-c-300ns and UE speed= 30 kmph.*

Figure 37, shows that CSI-IM based interference measurement has an overall higher performance compared to NZP CSI-RS. It also shows that CSI-IM measurements outperform NZP CSI-RS based one, in two different channel conditions i.e. in frequency selective and non selective channels. This is because CSI-IM interference measurement method is measuring inteference directely on CSI-IM REs resulting in more accurate measurement compared to the residual method used in NZP CSI-RS based interfernce measurement.

4.5 System overhead study

In this section, system overhead is studied, where two channel models are assumed: 3GPP tdl-a-30ns and 3GPP tdl-c-300ns with UE speed of 3 kmph. Interference measurement is carried out using CSI-IM and NZP CSI-RS with configurations explained in Section 3.9. Two different systems are assumed and link level simulations are carried out to study system overhead. The first system is based on CSI-IM based interference measurement method, where NZP CSI-RS and CSI-IM REs are both used to get channel and interference measurements respectively. Serving cell is configured with 2 REs of NZP CSI-RS colliding with 4 REs of ZP CSI-RS of interfering cells (2 REs each) to get clean channel measurement. Interfering cells have also the same configuration for channel measurement purpose (CFG1).

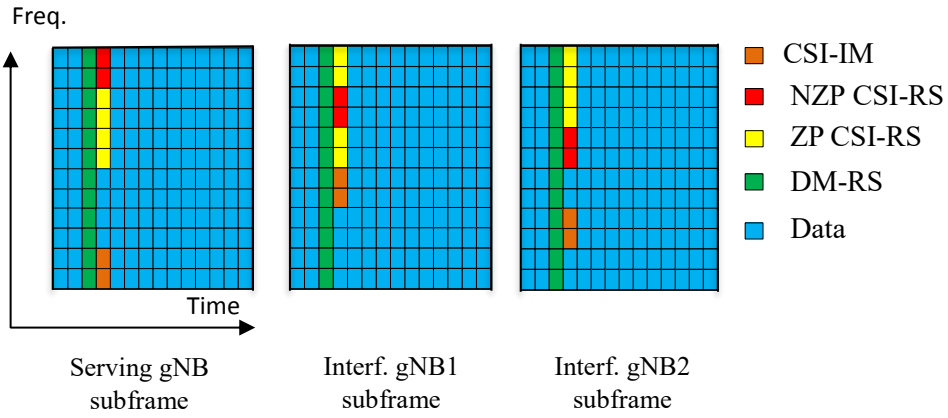

Figure 38. *First system (CFG1+CFG2)*

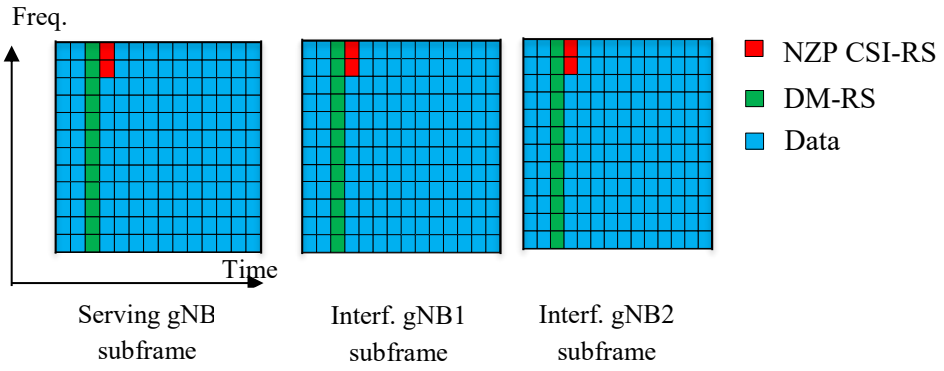

Figure 39. *Second system (CFG3)*

Interference measurement is carried out using 2 REs of CSI-IM signal colliding with data REs in interfering cells (CFG2). Figure 38, shows reference signals allocation in the subframe of serving and interfering cells. The total overhead for the first system is 4.76 % per PRB (8 REs/PRB). The second system is based on NZP CSI-RS interference measurement method where it uses only NZP CSI-RS to get both channel and interference measurements (CFG3). These REs are colliding with NZP CSI-RS resources of interfering cells. In this system, 2,4 and 6 NZP CSI-RS REs are evaluated resulting in system overhead of 1.19%, 2.38% and 3.57% respectively. Figure 39, shows NZP CSI-RS allocation within subframe of serving and interfering cells.

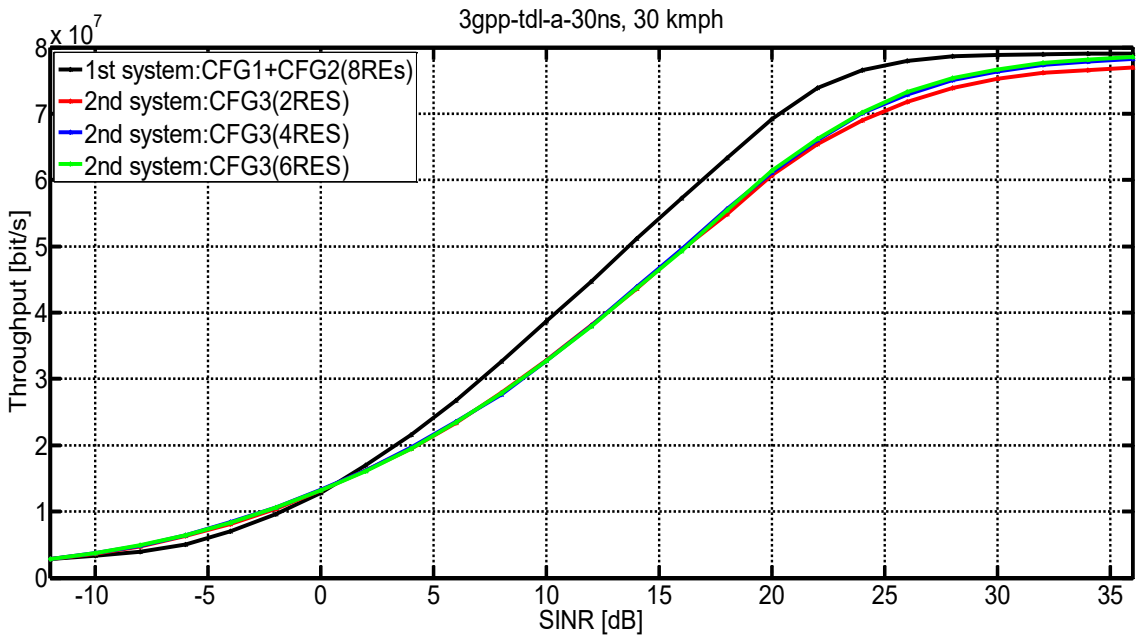

Figure 40. *System overhead analysis in frequency non-selective channel*

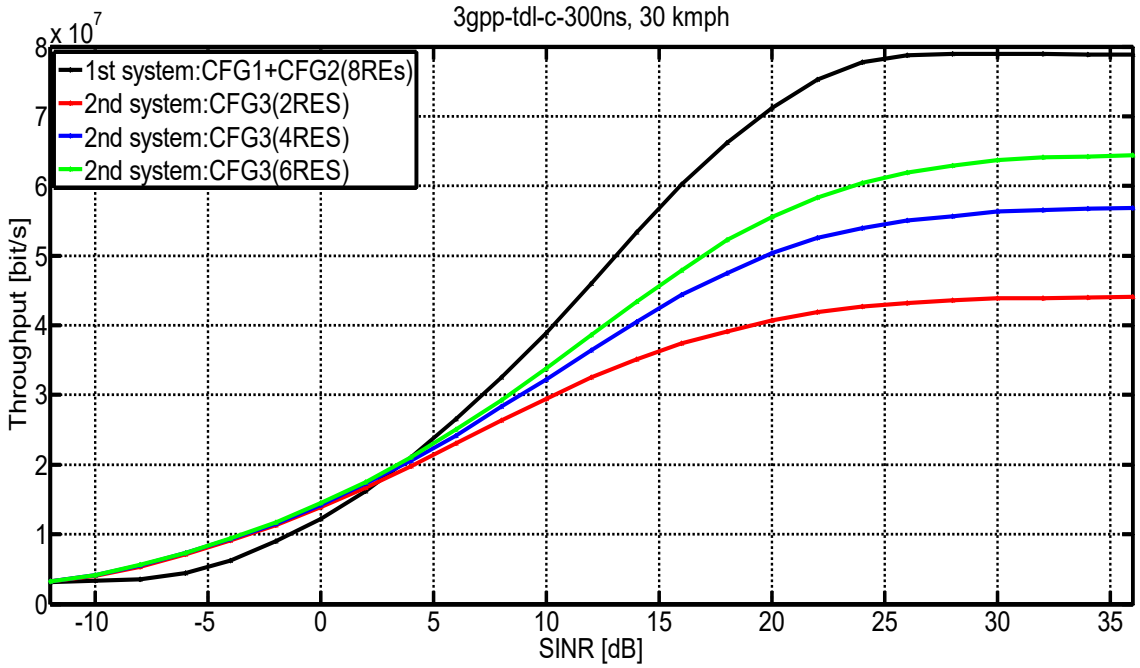

Figure 41. *System overhead analysis in frequency selective channel*

Figure 40, shows that in a frequency non-selective channel model that is 3GPP tdl-a-30ns, the first system has an overall better performance compared to the second system as explained in the previous section. However, it has higher system overhead of 4.76% compared to 1.19% system overhead in second system configured with of two NZP CSI-RS REs/PRB. On the other hand, figure 41 shows that in a frequency selective channel that is 3GPP tdl-c-300ns, the first system has an observable higher performance comapred to the second system. This comes with the price of higher system overhead. So, in general there is a trade-off between system performance and system overhead.

5. CONCLUSION

Interference measurement is an essential part of UE receiver and strongly affects the system performance. It is used in interference cancellation in data demodulation and to calculate CQI as a part of CSI reports. In this thesis, two RS-based interference measurement methods are evaluated through extensive link level simulations. CSI-IM and NZP CSI-RS are the reference signals studied. Measurements are carried out by UE on the cell edge with two interfering cells. Two different channel and interference measurement configurations are evaluated to study overall system overhead. Next, final remarks and observations drawn from results in Chapter 4 are introduced.

5.1 Observations and final remarks

In this thesis, the performance of CSI-IM and NZP CSI-RS based interference measurement methods is studied. The following findings are obtained:

CSI-IM based interference measurement method results shows that: in strong interference scenarios, full interference plus noise covariance matrix is the best mathematical representation to accurately capture interference characteristics in frequency and spatial domains. CSI-IM signal periodicity can be increased as long as it is reported within channel coherence time (T_c). This can be used to reduce system overhead. In higher mobility cases where T_c becomes smaller, CSI reports periodicities higher than T_c will have the same performance since outdated reports are used in gNB. Moreover, increasing number of CSI-IM REs per PRB will not improve interference measurement quality, since the frequency separation between CSI-IM REs is less than channel coherence bandwidth. This means that the measured interference is following the channel variations of interfering cells. Finally, CSI-IM frequency domain granularity (FG) can be reduced to every second PRB. However further reduction in FG will result in observable performance drop.

NZP CSI-RS based interference measurement method results shows that: in a time selective channel conditions, allocating NZP CSI-RS REs in one OFDM symbol is not enough to get accurate interference measurement due to fast varying channel conditions of interfering cells. This will result in observable performance drop. Scheduling CSI reports with periodicities higher than T_c, will result in outdated CQI in gNB. NZP CSI-RS based interference measurement has shown to be very sensitive to channel selectivity of interfering cells. Reducing FG of NZP CSI-RS signals will result in inaccurate interference measurement. Moreover, in frequency non-selective channel, 2 REs per PRB are enough to get accurate interference measurement. However, in frequency selective channel more REs are needed per PRB to capture channel conditions in frequency domain.

Comparison between the two RS-based interference measurement methods shows that, CSI-IM based method outperforms NZP CSI-RS based one, which answers one of the main questions of this thesis. System overhead study shows that the first system with CSI-IM signal used to get interference measurements results in observable better performance compared to the second system. This comes with the price of higher system overhead. In general, there is a trade-off between system performance and system overhead.

To summarize, two RS-based interference measurement methods are studied, and CSI-IM has proven to be more efficient and operates well in different channel scenarios and different UE speed, while NZP CS-RS shows sensitivity in case of frequency selective channel and higher user mobility cases. From overall system overhead perspective, CSI-IM based method is the best solution.

REFERENCES

[1] High Efficiency Video Coding, document Rec. H.265, ITU-T SG13, Apr. 2013.

[2] Mansoor Shafi *et al., "5G: A Tutorial Overview of Standards, Trials, Challenges, Deployment, and Practice"*. IEEE journal on selected areas in communications, vol. 35, no. 6, June 2017.

[3] Stefan Parkvall *et al*., "*NR: The New 5G Radio Access Technology*". IEEE Communications Standards Magazine, Volume: 1, Issue: 4, Dec. 2017.

[4] Qualcomm whitepaper, *"Making 5G NR a reality"*. December 2016. Online*: https://www.qualcomm.com/documents/whitepaper-making-5g-nr-reality.*

[5] Ali A. Zaidi *et al., "Waveform and Numerology to Support 5G services and Requirements".* IEEE Communications Magazine. November 2016.

[6] Andreas F. Molisch, *"Wireless Communications"*. Second Edition, United Kingdom 2011, John Wiley & Sons Ltd, 827 p.

[7] Zhouyue Pi *et al., "An Introduction to Millimeter-Wave Mobile Broadband Systems".* IEEE Communications Magazine. June 2011.

[8] Erik Dahlman, Stefan Parkvall, Johan Sköld, *"LTE/ LTE-Advanced for Mobile Broadband"*. Second edition 2014, Academic Press, 498 p.

[9] RP-160671, *"Study on NR New Radio Access Technology"* 3GPP TSG RAN, Meeting 71, Mar. 2016.

[10] 3GPP, Technical Specification 38.211, *"Physical Channels and Modulation". www.3gpp.org/specification-numbering,* version 15, Release 15.

[11] A. A. Zaidi *et al., "A Preliminary Study on Waveform Candidates for 5G Mobile Radio Communications above 6 GHz".* Proc. IEEE VTC-Spring, May 2016.

[12] 3GPP, Technical Report 38.802, *"Study on New Radio Access Technology Physical Layer Aspects".* www.3gpp.org/specification-numbering, version 14.2.0, Release 14.

[13] Alberto, Brihuega Garcia, *"Constant Envelope Precoding for Large Antenna Arrays".* Master of Science Thesis, August 2017.

[14] Ali A. Zaidi *et al.,* "*Designing for the future: the 5G NR physical layer"*. Ericsson

Technology Review, June 27, 2017.

[15] 3GPP, Technical Specification 38.101-1, *"User Equipment (UE) radio transmission and reception; part 1: range 1 standalone". www.3gpp.org/specification-numbering*, version 15.1, Release 15.

[16] Mikko, Mäenpää, *"Blind detection of interfering cell data channel power level in 3GPP LTE/LTE-Advanced downlink".* Master of Science Thesis, 12th of August 2015.

[17] Markku Renfors*, "Frequency-Domain Equalization and Single-Carrier Transmission in OFDM Framework".* lecture notes, Tampere University of Technology.

[18] Stefan Kaiser, *"Multi-carrier CDMA mobile radio systems analysis and optimization of detection, decoding and channel estimation"*. Ph.D. thesis published with: VDI-Verlag, Dusseldorf, Germany,1998.

[19] Nokia, Alcatel-Lucent Shanghai Bell, *"Interference estimation in NR".* 3GPP TSG RAN WG1#88 bis, R1-1705964, Spokane, WA, USA, 3rd - 7th April 2017.

[20] Panayiotis Papadimitriou *et al., "Link-level performance of an LTE UE Receiver in Synchronous and Asynchronous Networks".* IEEE Wireless Communications and Networking Conference (WCNC),2013.

[21] Ahmadi, Sassan *et.al., "LTE-Advanced: A Practical Systems Approach to Understanding 3GPP LTE Releases 10 and 11 Radio Access Technologies".* Elsevier Science & Technology, 2013.

[22] Vyacheslav Shumilov *et al*., "*Design of Link-to-System Mapping Interface for LTE-A Uplink System Level Simulations*". Lobachevsky State University of Nizhny Novgorod and Intel Corporation.

[23] MediaTek Inc., "*Text Proposal for TR36.863 for NAICS (Section 8)"* RAN4 contribution R4-134458.

[24] Severine Catreux *et al.,* "*Adaptive Modulation and MIMO Coding for Broadband Wireless Data Networks*". IEEE Communications Magazine. June 2002.

[25] Gosan Noh *et al*., "*DMRS Design and Evaluation for 3GPP 5G New Radio in a High Speed Train Scenario*". GLOBECOM 2017 - 2017 IEEE Global Communications Conference.

[26] 3GPP, Technical Specification 38.214, *"Physical layer procedures for data",* www.3gpp.org/specification-numbering, version 15.1, Release 15.

[27] A. Durán *et.al., "*Self-Optimization Algorithm for Outer Loop Link Adaptation in LTE". IEEE Communications Letters, Vol. 19, No. 11, November 2015

[28] 3GPP, RI-051334 (Motorola). *"CQI Feedback Scheme for EUTRA".* Seoul, Korea, November 2005.

[29] Muhammad Saad Akram, "*Pilot-based Channel Estimation in OFDM Systems"*, Master of Science Thesis, 6th of August 2007.

[30] J. G. Proakis and D. G. Manolakis, "*Digital Signal Processing - Principles, Algorithms, and Applications"*. Upper Saddle River, NJ: PrenticeHall, Inc., 1996.

[31] Yuanjie Wang *et.al.*, *"Performance Analysis of Interference Averaging for Link Adaptation in LTE/LTE-A Downlink"*, 2013 5th IEEE International Symposium on Microwave, Antenna, Propagation and EMC Technologies for Wireless Communications